

Space-Time-Doppler Block Coding for Correlated Time-Selective Fading Channels

Xiaoli Ma, *Member, IEEE*, Geert Leus, *Member, IEEE*, and Georgios B. Giannakis, *Fellow, IEEE*

Abstract—Coping with time-selective fading channels is challenging but also rewarding, especially with multiantenna systems, where joint space-Doppler diversity and coding gains can be collected to enhance performance of wireless mobile links. These gains have not been quantified, and space-time coded systems maximizing joint space-Doppler benefits have not been designed. Based on a parsimonious basis expansion model for the underlying time-selective (and possibly correlated) channels, we quantify these gains in closed form. Furthermore, we develop space-time-Doppler coded systems that guarantee the maximum possible space-Doppler diversity, along with the largest coding gains within all linearly coded systems. Our three novel designs exploit knowledge of the maximum Doppler spread, and each offers a uniquely desirable tradeoff, including high spectral efficiency, low decoding complexity, and high performance. Our analytical results are confirmed by simulations and reveal the relative of merits of our three designs in comparison with an existing approach.

Index Terms—Basis expansion channel model, diversity, fading, phase sweeping, space-time coding, time-varying channel.

I. INTRODUCTION

MODELING temporal channel variations and coping with time-selective fading are important and challenging tasks in mobile communications. Time-selectivity arises due to oscillator drifts, phase noise, multipath propagation, and relative motion between the transmitter and the receiver. In wireless mobile communications, time-variations and fading introduce selectivity in the time-domain, which in turn causes performance degradation. This motivates research toward efficient coding and modulation schemes that improve the reliability of information transmission over rapidly fading wireless links.

Manuscript received October 23, 2003; revised July 8, 2004. This work was prepared through collaborative participation in the Communications and Networks Consortium and supported by the U. S. Army Research Laboratory under the Collaborative Technology Alliance Program, Cooperative Agreement DAAD19-01-2-0011. The U. S. Government is authorized to reproduce and distribute reprints for Government purposes notwithstanding any copyright notation thereon. Part of the work in this paper was presented at the International Conference on Acoustics, Speech, and Signal Processing, Orlando, FL, May 13–17, 2002. The associate editor coordinating the review of this manuscript and approving it for publication was Prof. Zhi Ding.

X. Ma is with the Department of Electrical and Computer Engineering Auburn University, Auburn, AL 36849 USA (e-mail: xiaoli@eng.auburn.edu).

G. Leus is with the Faculty of Electrical Engineering, Mathematics, and Computer Science, Delft University of Technology, 2628CD Delft, The Netherlands (e-mail: leus@cas.et.tudelft.nl).

G. B. Giannakis is with the Department of Electrical and Computer Engineering, University of Minnesota, Minneapolis, MN 55455 USA (e-mail: georgios@ece.umn.edu).

Digital Object Identifier 10.1109/TSP.2005.847850

Traditionally, the popular approach to cope with fading has been to rely on diversity-enriched transmission and reception. Using multiple antennas, Space-Time (ST) coding offers such an approach and potentially boosts data rates when communicating over flat [4] or frequency-selective channels [1]. When transmissions are properly designed, quasistatic (constant over a block) frequency-selective channels offer also multipath diversity [13], [25], [26]. If, on the other hand, the channels are time-varying, judicious design of even single-antenna transmissions enables an additional diversity dimension, namely, *Doppler diversity* [15]. Joint exploitation of the ST and Doppler (STDO) diversity dimensions with multiple transmit-antennas is the goal of this paper.

The Doppler dimension can be induced naturally by time-selective channel effects, but it can also be injected intentionally to enhance diversity, or even introduce it, by a so-termed phase sweeping transmission that adds time-variations to an originally slow-fading channel [8], [11]. Unfortunately, the analog phase-sweeping-based approaches of [8], [11] consume extra bandwidth, and they are not designed to bring joint STDO benefits. The potential of STDO diversity was alluded to in [16], which dealt with quasistatic fading channels. An attempt to collect STDO gains was also made in [19] through the design of the so-called “smart-greedy” codes. Interestingly, although all existing works [8], [11], [16], [19] appreciated the importance of capitalizing on time-selectivity, none tailored its design to an explicit model of the underlying time-variations. STDO gains have not been quantified, and designs enabling the maximum STDO diversity provided by the channel along with large coding gains are missing.

The present paper fills these gaps by making use of an existing basis expansion model (BEM) [5], [15], which we adopt to capture parsimoniously the time-selective multiantenna channels. The basic idea behind our novel STDO coded designs is to utilize knowledge of the maximum Doppler spread at the transmitter. This key parameter that is readily measurable from the operational environment specifies all our multiantenna transmitters need to know about the BEM and allows us to quantify rigorously the maximum STDO diversity and coding gains. These gains benchmark the performance of STDO coded schemes in the presence of (even correlated) rapidly fading channels.

Equally important, the BEM facilitates our development and analysis of three STDO codecs. While we show that they are all capable of collecting the maximum STDO diversity, each offers a uniquely desirable tradeoff, including high spectral efficiency, low decoding complexity, and high coding gain. Our first STDO codec comprises a properly designed *digital* phase sweeping (DPS) scheme. Unlike [8] and [11], our DPS design renders the

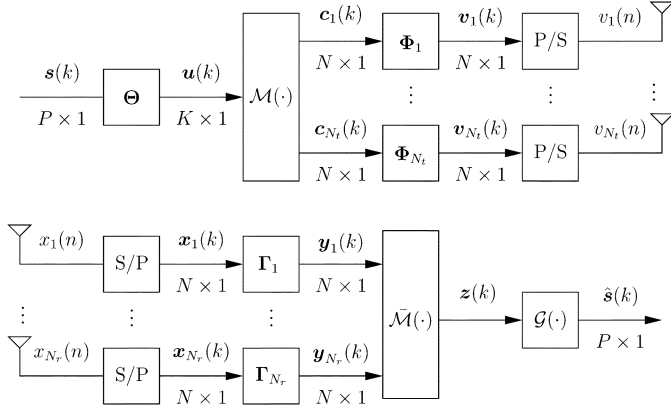


Fig. 1. Unifying discrete-time model of transmitter and receiver for STDO designs.

set of time-selective fading multi-antenna channels mathematically equivalent to a single combined faster channel offering the maximum joint STDO diversity. The other two STDO codecs are block orthogonal designs and emerge from a simple but neat duality property that we establish between the time-selectivity captured by the BEM and the frequency selectivity that is known to be approximated well by the finite impulse response (FIR) tapped delay line model. This duality property underpins our idea of transforming ST designs that have been developed for single- and multicarrier transmissions over frequency-selective channels [13], [25], [26] to our time-selective channels parameterized by the BEM.

The rest of the paper is organized as follows. Section II introduces our time-varying channel and the overall system model. In Section III, we provide a unifying description of our STDO designs and derive our performance criteria for STDO coding. Sections IV and V, respectively, deal with our digital phase sweeping and the block STDO codecs. Section VI verifies our BEM fitting results and confirms our STDO performance claims by simulations. Section VII concludes this paper.

Notation: Upper (lower) bold face letters will be used for matrices (column vectors). Superscript \mathcal{H} will denote Hermitian, $*$ conjugate, T transpose, and \dagger pseudo-inverse. We will reserve \otimes for the Kronecker product and $E[\cdot]$ for expectation. We will use $[\mathbf{A}]_{k,m}$ to denote the $(k+1, m+1)$ st entry of a matrix \mathbf{A} , $\text{tr}(\mathbf{A})$ for its trace, and $[\mathbf{x}]_m$ to denote the $(m+1)$ st entry of the column vector \mathbf{x} ; \mathbf{I}_N will denote the $N \times N$ identity matrix and \mathbf{F}_N the $N \times N$ normalized (unitary) FFT matrix; $\text{diag}[\mathbf{x}]$ will stand for a diagonal matrix with \mathbf{x} on its main diagonal.

II. PRELIMINARIES AND PROBLEM STATEMENT

We consider a wireless link with N_t transmit-antennas, N_r receive-antennas, and time-selective fading channels. Fig. 1 depicts the discrete-time equivalent baseband model under consideration.

A. Channel Model

Consider a multipath fading environment, where a number of reflected or scattered rays arrive at the receiving end with different delay, frequency offset, phase, and attenuation [17, p.

802]. If all rays arrive at the receiver almost simultaneously with a common propagation delay (that can be set to zero without loss of generality), then the channel experiences a time-selective nondispersive propagation. Let $h(t)$ denote the time-varying impulse response of the resulting channel that includes transmit-receive filters as well as time-selective propagation effects, and let $H(f)$ denote the Fourier transform of $h(t)$. Although the bandwidth of $h(t)$ over a finite time horizon is theoretically infinite, we practically have that $H(f) \approx 0$ for $f \notin [-f_{\max}, f_{\max}]$, where f_{\max} is the maximum frequency offset (Doppler shift) of all the rays. Considering that a block of N symbols with symbol period T_s is time-limited, we sample $H(f)$ along f with period $1/(NT_s)$, and collect $Q+1$ samples $\{H(q/(NT_s))\}_{q=-Q/2}^{Q/2}$, where $Q := 2\lceil f_{\max}T_sN \rceil$. Transforming these frequency-domain samples back to the time-domain and sampling along the time t , we obtain samples $h(n)$. Using the serial index n , we can describe the block index as $\lfloor n/N \rfloor$ and write our *discrete-time baseband equivalent channel* model as (see [15] for detailed derivations)

$$h(n) = \sum_{q=0}^Q h_q \left(\left\lfloor \frac{n}{N} \right\rfloor \right) e^{j\omega_q n} \quad (1)$$

where $\omega_q := 2\pi(q - Q/2)/N$, and $Q := 2\lceil f_{\max}T_sN \rceil$. Equation (1) constitutes our Basis Expansion Model (BEM). With $T_{k,0}$ denoting the initial time of the k th interval ($k := \lfloor n/N \rfloor$), the BEM represents $h(t)$ for $t \in [T_{k,0}, T_{k,0} + NT_s)$ using

- $Q+1$ coefficients $\{h_q(k)\}_{q=0}^Q$ that remain invariant per block, but are allowed to change with k ;
- $Q+1$ Fourier bases that capture even rapid time variations but are common $\forall k$.

Unlike [16], the complex exponential bases allow $h(n)$ to vary not only across blocks but also within every block. Notice also that the physical parameter dictating the BEM order Q is the Doppler spread f_{\max} , since N and T_s in $Q := 2\lceil f_{\max}NT_s \rceil$ are known to the designers.

Since the maximum Doppler shift f_{\max} can be measured experimentally from the maximum mobile speed and the carrier frequency in practice, we assume the following.

- Parameter f_{\max} is bounded and known.

Although not widely known, the finitely parameterized BEM for time-varying channels plays as important a role in the design of transmitters and receivers, as the FIR tapped delay line plays for time-invariant frequency-selective channels. Per block of N symbols, the BEM in (1) can be viewed either as deterministic or as the realization of a stochastic process with random coefficients $h_q(\lfloor n/N \rfloor)$. Within each block $k := \lfloor n/N \rfloor$, we will allow these coefficients to be correlated, but since we will work on a block-by-block basis, correlation across blocks will be irrelevant.

For time-selective channels, the Jakes' model has been widely adopted. However, from a channel estimation point of view, the Jakes' model is not as useful, because the number of parameters can be prohibitively large. In contrast, the BEM provides pragmatic description, which captures the main variations of time-selective channels. The finite parameterization of the BEM will allow us not only to quantify the STDO diversity but also

to devise multiantenna transmissions that achieve maximum diversity and coding gains.

B. Transmitter-Receiver Structure

The information-bearing symbols $\{s(n)\}$ are drawn from a finite alphabet \mathcal{A}_s and parsed into blocks of size $P \times 1$: $\mathbf{s}(k) := [s(kP), \dots, s((k+1)P-1)]^T$. Each block $\mathbf{s}(k)$ is linearly pre-coded by the $K \times P$ matrix Θ , resulting in $\mathbf{u}(k) := \Theta \mathbf{s}(k)$. This operation will be termed the outer STDO coding. Each block $\mathbf{u}(k)$ is further transformed into N_t blocks $\{\mathbf{c}_\mu(k)\}_{\mu=1}^{N_t}$ of size $N \times 1$ by a mapper $\mathcal{M}(\cdot)$: $\{\mathbf{c}_\mu(k)\}_{\mu=1}^{N_t} := \mathcal{M}(\mathbf{u}(k))$. This operation will be termed the middle STDO coding. Each block $\mathbf{c}_\mu(k)$ is finally linearly processed by the $N \times N$ matrix Φ_μ , resulting in $\mathbf{v}_\mu(k) := \Phi_\mu \mathbf{c}_\mu(k)$. This operation will be termed the inner STDO coding. Not all specific STDO designs will rely on all three (outer, middle, inner) stages of our unifying structure. If one, e.g., the inner stage is inactive, we will simply set $\Phi_\mu = \mathbf{I}_\mu$.

The sequence $v_\mu(n)$ obtained by parallel-to-serial converting the blocks $\{\mathbf{v}_\mu(k)\}$ is then pulse-shaped, carrier modulated, and transmitted from the μ th transmit-antenna. The n th sample at the ν th antenna's receive-filter output is

$$x_\nu(n) = \sum_{\mu=1}^{N_t} h^{(\nu,\mu)}(n)v_\mu(n) + \zeta_\nu(n), \quad \forall \nu \in [1, N_r] \quad (2)$$

where $h^{(\nu,\mu)}(n)$ is the time-selective channel response from the μ th transmit-antenna to the ν th receive-antenna (notice the channel dependence on n), and $\zeta_\nu(n)$ is complex additive white Gaussian noise (AWGN) at the ν th receive-antenna with mean zero and variance $\sigma_\zeta^2 = N_0$. According to (1), we have $h^{(\nu,\mu)}(n) := \sum_{q=0}^Q h_q^{(\nu,\mu)}(k)e^{j\omega_q(n)}$, $\forall \nu \in [1, N_r], \mu \in [1, N_t]$, where $\omega_q := 2\pi(q - Q/2)/N$, and $Q := 2\lceil f_{\max}NT_s \rceil$, as in (1).

At each receive-antenna, the symbol rate sampled sequence $x_\nu(n)$ at the receive-filter output is serial-to-parallel converted to form the $N \times 1$ blocks $[\mathbf{x}_\nu(k)]_n := x_\nu(kN + n)$. The matrix-vector counterpart of (2) can then be expressed as

$$\mathbf{x}_\nu(k) = \sum_{\mu=1}^{N_t} \mathbf{D}_H^{(\nu,\mu)}(k)\mathbf{v}_\mu(k) + \boldsymbol{\zeta}_\nu(k), \quad \forall \nu \in [1, N_r] \quad (3)$$

where $\mathbf{D}_H^{(\nu,\mu)}(k)$ is an $N \times N$ diagonal channel matrix that obeys the BEM

$$\mathbf{D}_H^{(\nu,\mu)}(k) := \sum_{q=0}^Q h_q^{(\nu,\mu)}(k)\mathbf{D}_q \quad (4)$$

with $\mathbf{D}_q := \text{diag}[1, \exp(j\omega_q), \dots, \exp(j\omega_q(N-1))]$ and the $\boldsymbol{\zeta}_\nu(k)$'s independent identically distributed (i.i.d.) AWGN noise vectors, which are defined similar to the $\mathbf{x}_\nu(k)$'s. Each block $\mathbf{x}_\nu(k)$ is linearly processed by the $N \times N$ matrix Γ_ν to yield $\mathbf{y}_\nu(k) := \Gamma_\nu \mathbf{x}_\nu(k)$. This operation is termed the inner STDO decoding. The blocks $\mathbf{y}_\nu(k)$ are further "demapped" to a block $\mathbf{z}(k)$ by $\bar{\mathcal{M}}(\cdot)$: $\mathbf{z}(k) := \bar{\mathcal{M}}(\{\mathbf{y}_\nu(k)\}_{\nu=1}^{N_r})$. This operation is termed the middle STDO decoding. The block $\mathbf{z}(k)$ is finally decoded by $\mathcal{G}(\cdot)$ to obtain an estimate of $\mathbf{s}(k)$ as $\hat{\mathbf{s}}(k) := \mathcal{G}(\mathbf{z}(k))$. This operation is termed the outer STDO decoding.

In this paper, we will show how to design the inner, middle, and outer STDO coders and decoders in order to collect joint space-Doppler diversity. Since in the following we will work on a block-by-block basis, we will drop the block index k .

III. DESIGN AND PERFORMANCE CRITERIA

In this section, we will design criteria for our STDO coding. Our derivations are based on the following operating conditions.

- A2) BEM coefficients $h_q^{(\nu,\mu)}$ are zero-mean, complex Gaussian random variables.
- A3) Channel state information (CSI) is available at the receiver but unknown at the transmitter.
- A4) High signal-to-noise ratio (SNR) is considered for deriving the diversity and coding gains.

When transmissions experience rich scattering and no line-of-sight is present, the central limit theorem validates A2). Notice that we allow not only for independent random channel coefficients but also for spatial and/or temporally correlated ones within each block.

Let us consider the best performance possible with STDO coded transmissions. Similar to [11], [17], [19], we will resort to the pairwise error probability (PEP) to define our optimality criteria. Define the PEP $P(\mathbf{s} \rightarrow \mathbf{s}' | \mathbf{D}_H^{(\nu,\mu)})$, $\forall \nu, \mu$ as the probability that maximum likelihood (ML) decoding of \mathbf{s} erroneously decides \mathbf{s}' instead of the actually transmitted \mathbf{s} . Conditioned on the $\mathbf{D}_H^{(\nu,\mu)}$'s, the Chernoff bound yields [17, p. 456]:

$$P(\mathbf{s} \rightarrow \mathbf{s}' | \mathbf{D}_H^{(\nu,\mu)}, \forall \nu, \mu) \leq \exp\left(-\frac{d^2(\tilde{\mathbf{x}}, \tilde{\mathbf{x}}')}{4N_0}\right) \quad (5)$$

where $\tilde{\mathbf{x}} := \left[\left(\sum_{\mu=1}^{N_t} \mathbf{D}_H^{(1,\mu)} \mathbf{v}_\mu \right)^T, \dots, \left(\sum_{\mu=1}^{N_t} \mathbf{D}_H^{(N_r,\mu)} \mathbf{v}_\mu \right)^T \right]^T$, the distance in the exponent is $d^2(\tilde{\mathbf{x}}, \tilde{\mathbf{x}}') = \sum_{\nu=1}^{N_r} \left\| \sum_{\mu=1}^{N_t} \mathbf{D}_H^{(\nu,\mu)} \mathbf{e}_\mu \right\|^2 = \mathbf{h}^H \mathbf{A}_e \mathbf{h}$, $\mathbf{h} = [h_0^{(1,1)}, \dots, h_Q^{(N_r, N_t)}]^T$, \mathbf{A}_e depends on \mathbf{e}_μ and the bases (see Appendix A for details), and $\mathbf{e}_\mu := \mathbf{v}_\mu - \mathbf{v}'_\mu$. Since our analysis will allow for correlated channels, we will denote the channel correlation matrix and its rank, respectively, by

$$\mathbf{R}_h := \mathbb{E}[\mathbf{h}\mathbf{h}^H], \text{ and } r_h := \text{rank}(\mathbf{R}_h) \leq N_t N_r (Q+1). \quad (6)$$

Eigenvalue decomposition of \mathbf{R}_h yields $\mathbf{R}_h = \mathbf{U}_h \boldsymbol{\Lambda}_h \mathbf{U}_h^H$. By defining

$$\boldsymbol{\Psi}_e := \left(\mathbf{U}_h \boldsymbol{\Lambda}_h^{1/2} \right)^H \mathbf{A}_e \mathbf{U}_h \boldsymbol{\Lambda}_h^{1/2} \quad (7)$$

$d^2(\tilde{\mathbf{x}}, \tilde{\mathbf{x}}')$ can be rewritten in terms of the eigenvalues of the matrix $\boldsymbol{\Psi}_e$ as $d^2(\tilde{\mathbf{x}}, \tilde{\mathbf{x}}') = \sum_{m=0}^{r_h-1} \lambda_m |\tilde{h}_m|^2$, where the λ_m 's are the eigenvalues of $\boldsymbol{\Psi}_e$, and the $|\tilde{h}_m|^2$'s have independent unit-mean Rayleigh distribution.

Since we wish our STDO coders to be independent of the particular channel realization, it is appropriate to average the PEP over the independent Rayleigh distributed $|\tilde{h}_m|^2$'s. If $r_e := \text{rank}(\boldsymbol{\Psi}_e)$, then r_e eigenvalues of $\boldsymbol{\Psi}_e$ are nonzero; without loss of generality, we denote these eigenvalues as $\lambda_0 \geq \dots \geq \lambda_{r_e-1}$.

At high SNR, the resulting average PEP is bounded as follows (see e.g., [15], [17]):

$$\bar{P}(\mathbf{s} \rightarrow \mathbf{s}') \leq \prod_{m=0}^{r_e-1} \left(\frac{\lambda_m}{4N_0} \right)^{-1} = \left(G_{e,c} \frac{1}{4N_0} \right)^{-G_{e,d}} \quad (8)$$

where $G_{e,d} := r_e$ is the diversity order, and $G_{e,c} := \left(\prod_{m=0}^{r_e-1} \lambda_m \right)^{1/r_e}$ is the coding gain for the error pattern $\mathbf{e} := \mathbf{s} - \mathbf{s}'$. Accounting for all possible pairwise errors, the diversity and coding gains for our STDO multiantenna systems are defined, respectively, as

$$G_d := \min_{\mathbf{e} \neq \mathbf{0}} G_{e,d}, \text{ and } G_c := \min_{\mathbf{e} \neq \mathbf{0}} G_{e,c}. \quad (9)$$

Because the performance of STDO depends on both G_d and G_c , it is important to maximize both of them, but before specializing to particular STDO designs that accomplish this, we wish to quantify the maximum possible G_d and G_c supplied by our BEM.

Equation (8) discloses that G_d depends on the rank r_e of Ψ_e . As the rank can not exceed the dimensionality, checking the dimensionality of Ψ_e , we recognize that the maximum diversity gain is given by

$$G_d^{\max} = r_h \leq N_t N_r (Q + 1) \quad (10)$$

and it is possible to achieve G_d^{\max} if and only if the matrix Ψ_e in (7) has full rank $r_h, \forall \mathbf{e} \neq \mathbf{0}$.

It is well known that at reasonably high SNR, the diversity order plays a more important role than the coding gain when it comes to improving the performance in wireless fading channels [19]. Thus, our STDO coding will focus on maximizing the diversity order first and then improving the coding gain as much as possible. Equation (8) also indicates that $G_{e,c}$ is the product of the nonzero eigenvalues of Ψ_e . It is not easy, however, to express G_c in closed form, but we can benchmark it when \mathbf{R}_h has full rank $N_r N_t (Q + 1)$.

Since \mathbf{R}_h is not known at the transmitter, we will allocate the transmit-power equally to the N_t substreams corresponding to the N_t transmit-antennas. For this reason, we set

$$E[\mathbf{v}_\mu^H \mathbf{v}_\mu] = \frac{1}{N_t} E[\mathbf{s}^H \mathbf{s}] = \frac{P}{N_t} \sigma_s^2 \quad (11)$$

where σ_s^2 is the power per information symbol. If the mapping from \mathbf{s} to \mathbf{v}_μ satisfies

$$\mathbf{v}_\mu = \sum_{p=0}^{P-1} \mathbf{a}_p^{(\mu)} [\mathbf{s}]_p + \mathbf{b}_p^{(\mu)} [\mathbf{s}]_p^*, \quad \forall \mu \in [1, N_t] \quad (12)$$

where $\mathbf{a}_p^{(\mu)}$ and $\mathbf{b}_p^{(\mu)}$ are $N \times 1$ vectors, then we call this ST transmitter a *linearly coded*¹ one. In Appendix A, we prove that the maximum coding gain for these linearly coded systems when \mathbf{R}_h has full rank $r_h = N_r N_t (Q + 1)$ is

$$G_c^{\max} = (\det(\mathbf{R}_h))^{1/r_h} \frac{d_{\min}^2}{N_t} \quad (13)$$

¹This general class was considered also in [7] when designing capacity maximizing linear dispersion ST-coded transmissions over flat-fading channels.

where d_{\min} is the minimum Euclidean distance of the constellation points in the finite alphabet \mathcal{A}_s .

In deriving performance bounds, we have assumed ML decoding, which comes with high computational complexity. Therefore, when we design the STDO encoders to guarantee the maximum diversity order, we will keep in mind the need to reduce decoding complexity while preserving the optimality in decoding. Before we proceed to design STDO coders, we summarize our results so far in the following proposition.

Proposition 1: Consider (N_t, N_r) multiantenna transmissions through time-selective channels adhering to a BEM as in (1) with $Q + 1$ bases. If the correlation matrix of the channel coefficients in (6) has rank r_h , then the maximum diversity order of transmissions in (3) is $G_d^{\max} = r_h \leq N_t N_r (Q + 1)$. For linearly coded systems, if \mathbf{R}_h has full rank $r_h = N_r N_t (Q + 1)$, then the maximum coding gain is $G_c^{\max} = (\det(\mathbf{R}_h))^{1/r_h} d_{\min}^2 / N_t$.

Notice that Proposition 1 provides a nice theoretical framework to justify, corroborate, and benchmark the results in [8], [11], [16]. However, it does not tell how to achieve this desirable maximum diversity and large coding gains. In the following two sections, we will provide three schemes, which enable the maximum STDO diversity and large coding gains.

IV. DIGITAL PHASE SWEEPING—FROM MIMO TO SISO

The first design that we study can be viewed as the *dual* of delay-diversity [18], which was originally developed for converting ST frequency-flat channels into a single frequency-selective channel. We will rely on the property that DPS can convert ST time-selective channels into a single faster time-selective channel. The analog phase sweeping (a.k.a. intentional frequency offset) idea was introduced in [8] and was later on combined with channel coding to further improve performance in [11]. The two transmit-antenna analog implementation modulates the signal of one antenna with a sweeping frequency f_s in addition to the carrier frequency f_c , which is present in both antennas [8], [11]. This causes bandwidth expansion. Furthermore, without an explicit channel model, [8] and [11] are unable to quantify diversity and coding gains.

A. DPS Encoding

For the DPS method, the middle STDO encoder $\mathcal{M}(\cdot)$ is just a power splitter (see Fig. 1). By equally allocating the signal power, we obtain $\mathbf{c}_\mu = \mathbf{u} / \sqrt{N_t}, \forall \mu \in [1, N_t]$. This means that for DPS, we have $K = N$. Using (3), \mathbf{x}_ν and \mathbf{s} can then be related via

$$\mathbf{x}_\nu = \frac{1}{\sqrt{N_t}} \sum_{\mu=1}^{N_t} \mathbf{D}_H^{(\nu, \mu)} \Phi_\mu \Theta \mathbf{s} + \zeta_\nu, \quad \nu \in [1, N_r]. \quad (14)$$

Observing (4), we notice that different channels share the same exponential bases, but they have different channel coefficients. Suppose that we shift the $Q + 1$ bases of each channel corresponding to one of the N_t transmit antennas so that all the bases are consecutive on the fast Fourier transform (FFT) grid of complex exponentials, as shown in Fig. 2 for $Q + 1 = N_t = 3$. Then, we can view the N_t channels to each receive-antenna as one equivalent time-selective channel with $N_t(Q + 1)$ bases. To

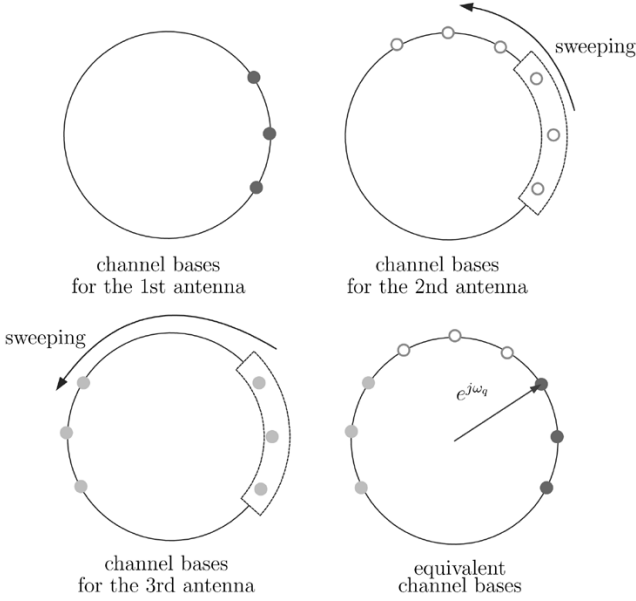


Fig. 2. DPS illustration. Black, hollow, and gray circles are shifted FT bases from three channels.

realize this intuition, we select the matrices $\{\Phi_\mu\}_{\mu=1}^{N_t}$, which determine the inner STDO encoder, as

$$\Phi_\mu = \text{diag}[1, e^{j\phi_\mu}, \dots, e^{j\phi_\mu(N-1)}], \quad \forall \mu \in [1, N_t]$$

where $\phi_\mu = 2\pi(\mu-1)(Q+1)/N$. As $\Phi_1 = \mathbf{I}$, the exponentials of the channel corresponding to the first ($\mu = 1$) transmit antenna remain unchanged, but those corresponding to the second channel ($\mu = 2$) are shifted from their original location in $\{\mathbf{D}_q\}_{q=0}^Q$ to $\{\mathbf{D}_q\}_{q=Q+1}^{2Q+1}$ after multiplication with the DPS matrix Φ_2 , which takes place at the second transmit-antenna, i.e., $\{\mathbf{D}_q\Phi_2\}_{q=0}^Q = \{\mathbf{D}_q\}_{q=Q+1}^{2Q+1}$. Proceeding likewise with all N_t DPS matrices, it follows that (14) can be rewritten as

$$\mathbf{x}_\nu = \frac{1}{\sqrt{N_t}} \sum_{q=0}^{N_t(Q+1)-1} h_q^{(\nu)} \mathbf{D}_q \Theta \mathbf{s} + \zeta_\nu, \quad \forall \nu \in [1, N_r] \quad (15)$$

where $h_q^{(\nu)} := h_{q \bmod (Q+1)}^{(\nu, \lfloor q/(Q+1) \rfloor + 1)}$. Comparing (14) with (15), we arrive at Fig. 2.

Property 1: DPS converts the N_t transmit-antenna system, where each channel can be expressed via $Q+1$ exponential bases to a single transmit-antenna system, where the equivalent channel is expressed by $N_t(Q+1)$ exponential bases.

Notice that since Φ_μ operates in the digital domain, the sweeping wraps the phases around $[-\pi, \pi)$, which explains why DPS does not incur bandwidth expansion.

Remark 1: To avoid overlapping the shifted bases, we should make sure that $N > N_t(Q+1)$. As for each receive-antenna, we have $N_t(Q+1)$ unknown BEM coefficients corresponding to N_t channels every N symbols. This condition guarantees that the number of unknowns is less than the number equations. Therefore, even from a channel estimation point of view, this condition is reasonable.

With the equivalence established by Property 1, our outer STDO codec, which is determined by Θ and $\mathcal{G}(\cdot)$, can be any

single-input codec that achieves the maximum diversity gain for the single transmit-antenna time-selective channels corresponding to each receive-antenna. From [15, Prop. 2], we know that ML decoding by means of $\mathcal{G}(\cdot)$ achieves the maximum diversity gain r_h if the linear precoder Θ is designed in such a way that $\Theta \mathbf{e}$ has at least $N_t(Q+1)$ nonzero entries for all possible error vectors $\mathbf{e} = \mathbf{s} - \mathbf{s}' \neq \mathbf{0}$. However, ML decoding for the entire $N \times 1$ block entails high computational complexity. To reduce the decoding complexity, we will split the design of the outer STDO encoder Θ in groups of smaller size.

Grouped Linear Constellation Precoded (GLCP) orthogonal frequency division multiplexing (OFDM) was proposed in [12] for single-antenna transmissions over frequency-selective channels. It provides one with a means of reducing decoding complexity without sacrificing the PEP-benchmarked performance. Here, we will design the outer STDO encoder Θ by adjusting this GLCP approach to our BEM for time-selective channels. Toward this objective, we select the transmitted block size $N = N_g N_{\text{sub}}$ and demultiplex the information vector \mathbf{s} into N_g groups: $\{\mathbf{s}_g\}_{g=0}^{N_g-1}$. Each group has length N_{sub} and contains the symbols collected in a vector \mathbf{s}_g as follows:

$$\mathbf{s}_g = [[\mathbf{s}]_{N_{\text{sub}}g}, \dots, [\mathbf{s}]_{N_{\text{sub}}(g+1)-1}]^T, \quad \forall g \in [0, N_g - 1]. \quad (16)$$

Correspondingly, we define the linearly precoded block of the g th group as

$$\mathbf{u}_g = \Theta_{\text{sub}} \mathbf{s}_g, \quad \forall g \in [0, N_g - 1] \quad (17)$$

where Θ_{sub} is an $N_{\text{sub}} \times N_{\text{sub}}$ matrix. To enable the maximum diversity, we select Θ_{sub} from the algebraic designs of [23]. The overall transmitted block \mathbf{u} consists of multiplexed subblocks $\{\mathbf{u}_g\}_{g=0}^{N_g-1}$ as follows:

$$\mathbf{u} = [\mathbf{u}_0]_0, \dots, [\mathbf{u}_{N_g-1}]_0, \dots, [\mathbf{u}_{N_g-1}]_{N_{\text{sub}}-1}]^T. \quad (18)$$

Notice that \mathbf{u} can be obtained from $\{\mathbf{u}_g\}_{g=0}^{N_g-1}$'s via a block interleaver with depth N_{sub} . Equivalently, we can relate \mathbf{u} with \mathbf{s} as

$$\mathbf{u} = \Theta \mathbf{s}, \quad \text{with } \Theta := \begin{bmatrix} \mathbf{I}_{N_g} \otimes \theta_1^T \\ \vdots \\ \mathbf{I}_{N_g} \otimes \theta_{N_{\text{sub}}}^T \end{bmatrix} \quad (19)$$

where θ_m^T is the m th row of Θ_{sub} , and \otimes denotes the Kronecker product. Equations (16)–(18) or, equivalently, (19) summarize our STDO transmitter design based on DPS.

To collect full diversity and large coding gains, we not only need to design the transmitter properly, but we must also select a proper decoder at the receiver.

B. DPS Decoding

Following the ‘‘reverse order’’ of DPS encoding, we start from the inner decoder. The inner decoder for the ν th receive antenna is designed as $\mathbf{T}_\nu = \mathbf{I}_N$, $\forall \nu \in [1, N_r]$. Hence, in the unifying block diagram of Fig. 1, we have $\mathbf{y}_\nu = \mathbf{x}_\nu$, $\forall \nu \in [1, N_r]$. Let

us denote the equivalent faster single transmit-antenna channel matrix as

$$\mathbf{D}_H^{(\nu)} = \sum_{q=0}^{N_t(Q+1)-1} h_q^{(\nu)} \mathbf{D}_q, \quad \forall \nu \in [1, N_r]. \quad (20)$$

Since the received blocks \mathbf{y}_ν from all N_r receive-antennas contain the information block \mathbf{s} , we need to combine the information from all received blocks to decode \mathbf{s} . To retain decoding optimality, we choose the maximum ratio combining (MRC) method. The MRC for $\mathbf{x}_\nu = \mathbf{y}_\nu$ in (15), amounts to selecting the middle decoder $\bar{\mathcal{M}}(\cdot)$ as [cf. (20)]

$$\mathbf{G} = \left(\sum_{\nu=1}^{N_r} \mathbf{D}_H^{(\nu)} \left(\mathbf{D}_H^{(\nu)} \right)^* \right)^{-1/2} \left[\left(\mathbf{D}_H^{(1)} \right)^* \dots \left(\mathbf{D}_H^{(N_r)} \right)^* \right]. \quad (21)$$

Existence of the inverse in (21) requires (only for the DPS design) the channels to satisfy the following.

A5) Channels $\mathbf{D}_H^{(\nu)}$ are coprime, i.e., $\det \left(\sum_{\nu=1}^{N_r} \mathbf{D}_H^{(\nu)} \left(\mathbf{D}_H^{(\nu)} \right)^* \right) \neq 0$.

Assumption A5) is more technical rather than restrictive since it requires that not all equivalent channels are identically zero at the same time slot. For random channels, A5) excludes an event with probability measure zero.

With the MRC of (21), the output \mathbf{z} of $\bar{\mathcal{M}}(\cdot)$ is given by

$$\mathbf{z} = \mathbf{G} \begin{bmatrix} \mathbf{y}_1 \\ \vdots \\ \mathbf{y}_{N_r} \end{bmatrix} = \frac{1}{\sqrt{N_t}} \left(\sum_{\nu=1}^{N_r} \mathbf{D}_H^{(\nu)} \left(\mathbf{D}_H^{(\nu)} \right)^* \right)^{1/2} \boldsymbol{\Theta} \mathbf{s} + \boldsymbol{\eta} \quad (22)$$

where $\boldsymbol{\eta} := \mathbf{G} [\boldsymbol{\zeta}_1^T, \dots, \boldsymbol{\zeta}_{N_r}^T]^T$. Thanks to A5), it can be verified that \mathbf{G} satisfies $\mathbf{G}\mathbf{G}^H = \mathbf{I}$. Since the $\boldsymbol{\zeta}_\nu$'s are i.i.d. additive white Gaussian noise (AWGN) vectors, the noise vector $\boldsymbol{\eta}$ retains its whiteness.

Following MRC, we split \mathbf{z} into N_g groups:

$$\mathbf{z}_g = \frac{1}{\sqrt{N_t}} \mathbf{D}_{H,g} \boldsymbol{\Theta}_{\text{sub}} \mathbf{s}_g + \boldsymbol{\eta}_g, \quad \forall g \in [0, N_g - 1] \quad (23)$$

where $\mathbf{z}_g := [[\mathbf{z}]_g, [\mathbf{z}]_{N_{\text{sub}}+g}, \dots, [\mathbf{z}]_{N_{\text{sub}}(N_g-1)+g}]^T$, $\mathbf{D}_{H,g}$ is the corresponding diagonal submatrix from $\left(\sum_{\nu=1}^{N_r} \mathbf{D}_H^{(\nu)} \left(\mathbf{D}_H^{(\nu)} \right)^* \right)^{1/2}$ for the g th group, and $\boldsymbol{\eta}_g$ is the corresponding AWGN noise vector that is similarly defined as \mathbf{z}_g .

ML decoding by means of $\mathcal{G}(\cdot)$ can then be implemented by applying the Sphere Decoding (SD) algorithm [21] on sub-blocks of small size N_{sub} .

The performance of our DPS depends on the selection of the subblock size N_{sub} . When $N_{\text{sub}} \geq N_t(Q+1)$, the maximum diversity order in (10) is achieved.

We summarize our diversity and coding gain results for DPS in the following proposition (see Appendix B for a proof).

Proposition 2: The maximum achievable STDO diversity order $G_d = r_h$ is enabled by our DPS design when the group size is selected as $N_{\text{sub}} \geq N_t(Q+1)$. When the channel correlation matrix \mathbf{R}_h has full rank $r_h = N_r N_t(Q+1)$, our

DPS design enables also the maximum possible coding gain among all linearly coded transmissions that is given in closed form by $G_c^{\text{max}} = (\det(\mathbf{R}_h))^{1/r_h} d_{\text{min}}^2 / N_t$. Transmission rate 1 symbol/sec/Hz is achieved by this DPS design.

In fact, the group size N_{sub} controls the tradeoff between performance and decoding complexity. When $N_{\text{sub}} \leq N_t(Q+1)$, as N_{sub} decreases, the decoding complexity decreases, whereas at the same time, the diversity order decreases. By adjusting N_{sub} , we can balance the affordable complexity with the required performance.

The matrices $\{\Phi_\mu\}_{\mu=1}^{N_t}$ in (14) introduce digital phase sweeping in our block transmissions, which is reminiscent of that used in [8] and [11], to increase the variation (and, thus, the potential for diversity) of time-selective channels. The differences between our design and [8] are as follows.

- i) We generalize the phase sweeping idea to multiple transmit- and receive-antennas.
- ii) We collect not only space-diversity as in [8] but Doppler diversity as well.
- iii) DPS can be used not only for coded but for uncoded systems as well.
- iv) Our digital design does not consume extra bandwidth.
- v) Combined with GLCP, our DPS can afford low decoding complexity.

V. BLOCK STDO CODES

In this section, we follow a different approach to designing STDO codes for rapidly varying channels. The main idea here is to invoke the inner STDO codec to transform the time-selective channels into frequency-selective channels by means of FFT and IFFT operations. As middle and outer STDO encoder, we can then use any of the existing orthogonal Space-Time-Multipath (STM) designs to achieve the maximum diversity and large coding gains. In the following, we will first establish the duality between our finite basis expansion model for time-selective channels, and the popular finite impulse response (FIR) tapped delay line model for frequency-selective channels. Then, we will design two STDO coders based on their dual STM coders.

A. Time-Frequency Duality

It is well known that circulant matrices can be diagonalized by (I)FFT matrices [6, p. 202]. Using this property and recalling that the BEM in (4) has its bases on the FFT grid, we can rewrite $\mathbf{D}_H^{(\nu,\mu)}$ as

$$\mathbf{D}_H^{(\nu,\mu)} = \sum_{q=0}^Q h_q^{(\nu,\mu)} \mathbf{D}_q = \mathbf{F}_N \mathbf{H}^{(\nu,\mu)} \mathbf{F}_N^H \quad (24)$$

where $\mathbf{H}^{(\nu,\mu)}$ is a circulant $N \times N$ matrix with first column $[h_{Q/2}^{(\nu,\mu)} \dots h_0^{(\nu,\mu)} 0 \dots 0 h_Q^{(\nu,\mu)} \dots h_{Q/2+1}^{(\nu,\mu)}]^T$, and \mathbf{F}_N denotes the N -point FFT matrix with the $(m+1, n+1)$ st entry $[\mathbf{F}_N]_{m,n} = (1/\sqrt{N}) e^{-j2\pi mn/N}$. If we now design the inner STDO codec in Fig. 1 as

$$\Phi_\mu = \mathbf{F}_N, \quad \forall \mu \in [1, N_t], \text{ and } \Gamma_\nu = \mathbf{F}_N^H, \quad \forall \nu \in [1, N_r] \quad (25)$$

then based on (3), (24), and (25), we obtain

$$\begin{aligned} \mathbf{y}_\nu &= \mathbf{F}_N^H \mathbf{x}_\nu = \sum_{\mu=1}^{N_t} \mathbf{F}_N^H \mathbf{D}_H^{(\nu,\mu)} \mathbf{F}_N \mathbf{c}_\mu + \mathbf{F}_N^H \boldsymbol{\zeta}_\nu \\ &= \sum_{\mu=1}^{N_t} \mathbf{H}^{(\nu,\mu)} \mathbf{c}_\mu + \boldsymbol{\eta}_\nu, \quad \forall \nu \in [1, N_r]. \end{aligned} \quad (26)$$

It is well known that for transmissions over frequency-selective channels, one can insert (at the transmitter), and remove (at the receiver) a cyclic prefix (CP) to render the channel equivalent to a circulant matrix; see, e.g., [12], [25], and [26]. Then, the circulant matrix can be diagonalized by FFT and IFFT operations. Equations (24)–(26) suggest the converse direction; thanks to the BEM, it is possible to convert the diagonal time-selective channel $\mathbf{D}_H^{(\nu,\mu)}$ to a circulant matrix after IFFT and FFT operations. The $Q+1$ BEM coefficients are dual to the channel taps of a frequency-selective channel. Hence, the inner STDO codec is capable of transforming our multiantenna ST time-selective channels into ST frequency-selective channels.

In order to achieve the maximum diversity gain r_h , we can adopt some of the existing STM codecs as our middle and outer STDO codecs. In the following, we will design and analyze a *low-complexity* CP-based approach and a *high-performance* Zero Padding (ZP)-based approach.

B. CP-Based Approach

In this approach, we start by designing the middle STDO codec, which consists of two stages. The first stage implements ST block coding that is used to collect the spatial diversity. The second stage implements a GLCP-OFDM-based module to collect the Doppler (that can now be viewed as multipath) diversity.

The ST block coding stage comprises an extension of the generalized complex orthogonal design (GCOD) developed in [20] for flat channels to our time-selective channels. Consider splitting \mathbf{u} into N_s equally long subblocks of size N_{od} as the input of the GCOD, i.e., $K = N_s N_{od}$. Define the size of the output of the GCOD as $N_d N_{od}$. Therefore, the rate of the ST block code is N_s/N_d . Our ST block code matrix is

$$\mathbf{V}_{(N_d N_{od}) \times N_t} = \sum_{i=0}^{N_s-1} (\mathbf{A}_i \otimes \mathbf{u}_i + \mathbf{B}_i \otimes \mathbf{u}_i^*) \quad (27)$$

where $\mathbf{u}_i := [[\mathbf{u}]_{N_{od}i}, \dots, [\mathbf{u}]_{N_{od}(i+1)-1}]^T$, and the real matrices $\{\mathbf{A}_i \in \mathbb{R}^{N_d \times N_t}, \mathbf{B}_i \in \mathbb{R}^{N_d \times N_t}, \forall i \in [0, N_s-1]\}$ satisfy the following properties:

$$\mathbf{A}_i^T \mathbf{A}_{i'} + \mathbf{B}_i^T \mathbf{B}_{i'} = \frac{1}{N_t} \mathbf{I}_{N_t} \delta(i-i'), \text{ and } \mathbf{A}_i^T \mathbf{B}_{i'} = \mathbf{0}. \quad (28)$$

The symbols of the μ th column of \mathbf{v} are directed to the μ th transmit-antenna.

Thanks to the FFT inner codec, the time-selective channel is converted to a frequency-selective channel. Dealing now with a frequency-selective channel, the second stage of our middle

STDO codec forms an OFDM-based block transmission (similar to [12]). After the first stage of ST block coding, we perform an IFFT and add a cyclic-prefix (CP)² to each subblock with length N_{od} , i.e., N_{od} subcarriers for each OFDM symbol. In matrix form, these operations can be described as

$$[\mathbf{c}_1 \dots \mathbf{c}_{N_t}] = \rho (\mathbf{I}_{N_d} \otimes \mathbf{T}_{cp}) (\mathbf{I}_{N_d} \otimes \mathbf{F}_{N_{od}}^H) \mathbf{V}$$

where $\rho = \sqrt{N_{od}/(N_{od}+Q)}$ is a power-normalizing constant, and $\mathbf{T}_{cp} := [\mathbf{T}_1, \mathbf{I}_{N_{od}}, \mathbf{T}_2]^T$ is a matrix implementing the CP insertion, with

$$\begin{aligned} \mathbf{T}_1 &:= [\mathbf{0}_{(Q/2) \times (N_{od}-Q/2)}, \mathbf{I}_{Q/2}]^T \\ \text{and } \mathbf{T}_2 &:= [\mathbf{I}_{Q/2}, \mathbf{0}_{(Q/2) \times (N_{od}-Q/2)}]^T. \end{aligned}$$

Correspondingly, at the receiver, we design the middle STDO decoder $\bar{\mathcal{M}}(\cdot)$ following the reverse order of the two encoding stages. Specifically, we remove the CP and perform an FFT by premultiplying with $(\mathbf{I}_{N_d} \otimes \mathbf{F}_{N_{od}})(\mathbf{I}_{N_d} \otimes \mathbf{R}_{cp})$ the received block on each antenna, where $\mathbf{R}_{cp} := [\mathbf{0}_{N_{od} \times (Q/2)}, \mathbf{I}_{N_{od}}, \mathbf{0}_{N_{od} \times (Q/2)}]$ is a matrix description of the CP removal operation. Recalling (26), and our inner codec, we infer that the equivalent channel matrix facing the middle STDO codec is a circulant matrix $\mathbf{H}^{(\nu,\mu)}$. With the OFDM module, the equivalent channel becomes

$$\begin{aligned} (\mathbf{I}_{N_d} \otimes \mathbf{F}_{N_{od}})(\mathbf{I}_{N_d} \otimes \mathbf{R}_{cp}) \mathbf{H}^{(\nu,\mu)} (\mathbf{I}_{N_d} \otimes \mathbf{T}_{cp}) (\mathbf{I}_{N_d} \otimes \mathbf{F}_{N_{od}}^H) \\ = \mathbf{I}_{N_d} \otimes \bar{\mathbf{D}}_H^{(\nu,\mu)} \end{aligned} \quad (29)$$

where $\bar{\mathbf{D}}_H^{(\nu,\mu)} := \text{diag}[H^{(\nu,\mu)}(0), \dots, H^{(\nu,\mu)}(N_{od}-1)]$, and $H^{(\nu,\mu)}(m) := \sum_{q=0}^Q h_q^{(\nu,\mu)} e^{-j2\pi q/N_{od}m}$.

To decode the ST block code, we need to simplify our input–output relationship using (29). Based on (26) and (29), after CP removal and FFT processing, we obtain

$$\begin{aligned} \bar{\mathbf{y}}_\nu &:= (\mathbf{I}_{N_d} \otimes \mathbf{F}_{N_{od}})(\mathbf{I}_{N_d} \otimes \mathbf{R}_{cp}) \mathbf{y}_\nu \\ &= \rho \sum_{\mu=1}^{N_t} (\mathbf{I}_{N_d} \otimes \bar{\mathbf{D}}_H^{(\nu,\mu)}) [\mathbf{V}]_\mu \\ &\quad + (\mathbf{I}_{N_d} \otimes \mathbf{F}_{N_{od}})(\mathbf{I}_{N_d} \otimes \mathbf{R}_{cp}) \boldsymbol{\eta}_\nu \end{aligned}$$

where $[\mathbf{V}]_\mu$ stands for the μ th column of \mathbf{V} . Plugging $[\mathbf{V}]_\mu$ into (27), we rewrite $\bar{\mathbf{y}}_\nu$ as

$$\begin{aligned} \bar{\mathbf{y}}_\nu &= \rho \sum_{i=1}^{N_s} \left(\sum_{\mu=1}^{N_t} [\mathbf{A}_i]_\mu \otimes (\bar{\mathbf{D}}_H^{(\nu,\mu)} \mathbf{u}_i) \right. \\ &\quad \left. + \sum_{\mu=1}^{N_t} [\mathbf{B}_i]_\mu \otimes (\bar{\mathbf{D}}_H^{(\nu,\mu)} \mathbf{u}_i^*) \right) + \bar{\boldsymbol{\eta}}_\nu \end{aligned}$$

where $\bar{\boldsymbol{\eta}}_\nu := (\mathbf{I}_{N_d} \otimes \mathbf{F}_{N_{od}})(\mathbf{I}_{N_d} \otimes \mathbf{R}_{cp}) \boldsymbol{\eta}_\nu$, and $[\mathbf{A}_i]_\mu$ and $[\mathbf{B}_i]_\mu$ are the μ th columns of \mathbf{A}_i and \mathbf{B}_i , respectively.

²Actually, here, we add both a cyclic prefix and a cyclic suffix. Since the suffix has the same effect as the cyclic prefix in OFDM system, for convenience, we still call it cyclic prefix.

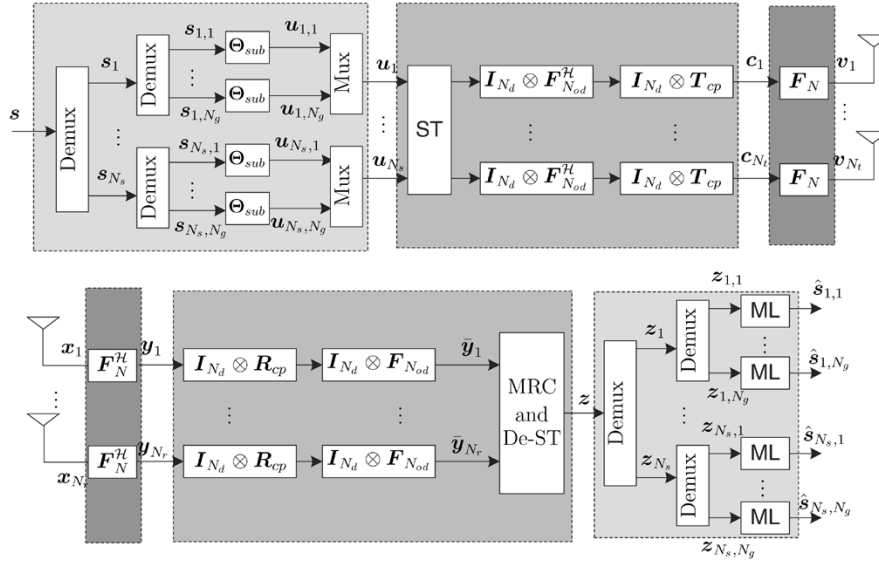


Fig. 3. CP-based STDO transceiver design.

Similar to the DPS decoding scheme in Section IV, we will rely on MRC to combine the received blocks from different antennas. Based on the orthogonality of \mathbf{A}_i 's and \mathbf{B}_i 's in (28), to implement the MRC, we use the combiner

$$\mathbf{G}_i = \sqrt{N_t} \left(\sum_{\nu=1}^{N_r} \sum_{\mu=1}^{N_t} \bar{\mathbf{D}}_H^{(\nu,\mu)} \left(\bar{\mathbf{D}}_H^{(\nu,\mu)} \right)^* \right)^{-1/2} \times \left[\mathbf{G}_i^{(1)}, \dots, \mathbf{G}_i^{(N_r)} \right]$$

where

$$\mathbf{G}_i^{(\nu)} = \left[\sum_{\mu=1}^{N_t} [\mathbf{A}_i]_{\mu}^T \otimes \left(\bar{\mathbf{D}}_H^{(\nu,\mu)} \right)^*, \sum_{\mu=1}^{N_t} [\mathbf{B}_i]_{\mu}^T \otimes \bar{\mathbf{D}}_H^{(\nu,\mu)} \right], \forall i \in [0, N_s - 1], \nu \in [1, N_r].$$

Here, for the CP-based scheme only, we need to modify A5) as follows:

$$\text{A5')} \text{ Channels } \bar{\mathbf{D}}_H^{(\nu,\mu)} \text{ are coprime, i.e., } \det \left(\sum_{\nu=1}^{N_r} \sum_{\mu=1}^{N_t} \left(\bar{\mathbf{D}}_H^{(\nu,\mu)} \bar{\mathbf{D}}_H^{(\nu,\mu)} \right)^* \right) \neq 0.$$

Under A5'), we have $\mathbf{G}_i \mathbf{G}_i^H = \mathbf{I}$. At the receiver, the i th sub-block corresponding to \mathbf{u}_i is

$$\begin{aligned} \mathbf{z}_i &= \mathbf{G}_i \left[\bar{\mathbf{y}}_1^T, \bar{\mathbf{y}}_1^H, \dots, \bar{\mathbf{y}}_{N_r}^T, \bar{\mathbf{y}}_{N_r}^H \right]^T \\ &= \rho \left(\sum_{\nu=1}^{N_r} \sum_{\mu=1}^{N_t} \bar{\mathbf{D}}_H^{(\nu,\mu)} \left(\bar{\mathbf{D}}_H^{(\nu,\mu)} \right)^* \right)^{1/2} \mathbf{u}_i + \boldsymbol{\xi}_i \end{aligned}$$

where $\boldsymbol{\xi}_i := \mathbf{G}_i \left[\bar{\boldsymbol{\eta}}_1^T, \bar{\boldsymbol{\eta}}_1^H, \dots, \bar{\boldsymbol{\eta}}_{N_r}^T, \bar{\boldsymbol{\eta}}_{N_r}^H \right]^T, \forall i \in [0, N_s - 1]$ is a circular AWGN vector.

The outer STDO encoder $\boldsymbol{\Theta}$ is designed as

$$\boldsymbol{\Theta} = \mathbf{I}_{N_s} \otimes \bar{\boldsymbol{\Theta}}.$$

The i th subblock is precoded by $\bar{\boldsymbol{\Theta}}$, i.e., $\mathbf{u}_i = \bar{\boldsymbol{\Theta}} \mathbf{s}_i, \forall i \in [0, N_s - 1]$. As in the DPS design, in order to reduce the decoding complexity, we again pursue the design of $\bar{\boldsymbol{\Theta}}$ in a grouped form.

Since the equivalent channel matrix between \mathbf{z}_i and \mathbf{s}_i is diagonal, we can write the g th group of \mathbf{z}_i , which is defined as $\mathbf{z}_{i,g}$, as

$$\mathbf{z}_{i,g} = \frac{\rho}{\sqrt{N_t}} \times \left(\sum_{\nu=1}^{N_r} \sum_{\mu=1}^{N_t} \bar{\mathbf{D}}_{H,g}^{(\nu,\mu)} \left(\bar{\mathbf{D}}_{H,g}^{(\nu,\mu)} \right)^* \right)^{1/2} \boldsymbol{\Theta}_{\text{sub}} \mathbf{s}_{i,g} + \boldsymbol{\xi}_{i,g} \quad (30)$$

where $\boldsymbol{\Theta}_{\text{sub}}$ is an $\bar{N}_{\text{sub}} \times \bar{N}_{\text{sub}}$ matrix designed according to [23] with $\bar{N}_{\text{sub}} = N_{od}/N_g$. Again, ML decoding for $\mathbf{s}_{i,g}$ can be performed by using sphere-decoding with block size \bar{N}_{sub} .

Based on (12), we can verify that our CP-based approach also constitutes a linearly coded transmission. When $N_{od} \geq (Q+1)$, the maximum diversity order r_h is enabled. Furthermore, when $r_h = N_r N_t (Q+1)$, and we select $\bar{N}_{\text{sub}} = Q+1$, the coding gain for this CP-based scheme satisfies [cf. (13)]

$$(\ln 2) \bar{G}_c \leq G_c \leq \bar{G}_c \quad (31)$$

where $\bar{G}_c = (\det(\mathbf{R}_h))^{1/r_h} (N_{od} d_{\min}^2 / (N_{od} + Q) N_t)$, and the upper bound \bar{G}_c is achieved when $\bar{N}_{\text{sub}} = Q+1$ satisfies a certain algebraic property [23].

The encoding and decoding processes of this CP-based approach are summarized in the block diagram of Fig. 3, and our results are collected in the following proposition (see Appendix C for a proof):

Proposition 3: CP-based STDO block codes enable the maximum space-Doppler diversity $G_d = r_h$, when $\bar{N}_{\text{sub}} \geq Q+1$, and offer low (FFT-based) sphere decoding complexity at the receiver. When the channel correlation matrix \mathbf{R}_h has full rank $N_t N_r (Q+1)$, the CP-based design achieves the maximum coding gain G_c^{max} of linearly coded systems, asymptotically, as N_{od} increases. The transmission rate of the CP-based design is $r_{\text{stbc}} N_{od} / (N_{od} + Q)$, where r_{stbc} is the rate of the corresponding block ST codes (specified in [20]).

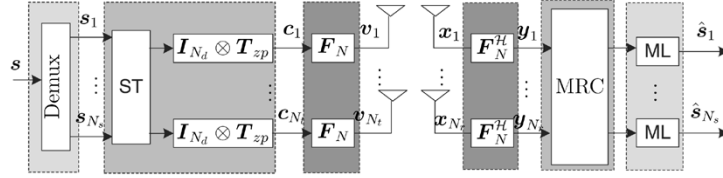


Fig. 4. ZP-based STDO transceiver design.

C. ZP-Based Approach

In this ZP-based approach, zero padding (ZP) replaces the CP guard. Similar to the CP-based design, there are two stages of the middle STDO codec. The first stage implements the GCOD, which is similar to (27), while the second eliminates inter-block interference (IBI) by padding zeros after each subblock.

As in Section V-B, we extend the scalar GCOD of [20] to the block based GCOD

$$\mathbf{V}_{N_d N_{od} \times N_t} = \sum_{i=0}^{N_s-1} [\mathbf{A}_i \otimes \mathbf{u}_i + \mathbf{B}_i \otimes (\mathbf{P}_1 \mathbf{u}_i^*)] \quad (32)$$

where \mathbf{u}_i is defined as in (32); \mathbf{P}_1 is a time-reversal matrix with entries $[\mathbf{P}_1]_{p,q} = \delta(p+q-N_{od}-1)$, and the matrices $\{\mathbf{A}_i \in \mathbb{R}^{N_d \times N_t}, \mathbf{B}_i \in \mathbb{R}^{N_d \times N_t}, \forall i \in [0, N_s-1]\}$ are defined as in (28). As for the second stage of the middle STDO encoder, instead of inserting the CP as in Section V-A, we insert leading and trailing zeros in each subblock. Based on the design of the inner codec in (25) and the middle STDO encoder, the input-output relationship from \mathbf{V} to \mathbf{y}_ν is

$$\mathbf{y}_\nu = \sum_{\mu=1}^{N_t} \mathbf{H}^{(\nu,\mu)} (\mathbf{I}_{N_d} \otimes \mathbf{T}_{zp}) [\mathbf{V}]_\mu + \boldsymbol{\eta}_\nu \quad (33)$$

where $\mathbf{T}_{zp} := [\mathbf{0}_{N_{od} \times Q/2} \mathbf{I}_{N_{od}} \mathbf{0}_{N_{od} \times Q/2}]^T$ implements the ZP insertion. We can verify that $\mathbf{H}^{(\nu,\mu)} (\mathbf{I}_{N_d} \otimes \mathbf{T}_{zp}) = \mathbf{I}_{N_d} \otimes (\bar{\mathbf{H}}^{(\nu,\mu)} \mathbf{T}_{zp})$, where the $(N_{od}+Q) \times (N_{od}+Q)$ circulant matrix $\bar{\mathbf{H}}^{(\nu,\mu)}$ has the same structure as $\mathbf{H}^{(\nu,\mu)}$. The outer STDO encoder $\boldsymbol{\Theta}$ is selected here to be an identity matrix, i.e., $\mathbf{u} = \mathbf{s}$.

At the receiver, to decode the ST block code and combine the results from different receive antennas, we use the MRC matrix

$$\mathbf{G}_i = \sqrt{N_t} \left(\sum_{\nu=1}^{N_r} \sum_{\mu=1}^{N_t} \bar{\mathbf{H}}^{(\nu,\mu)} (\bar{\mathbf{H}}^{(\nu,\mu)})^H \right)^{-1/2} \times [\mathbf{G}_i^{(1)}, \dots, \mathbf{G}_i^{(N_r)}] \quad (34)$$

where $\mathbf{G}_i^{(\nu)} = [\sum_{\mu=1}^{N_t} [\mathbf{A}_i]_\mu^T \otimes (\bar{\mathbf{H}}^{(\nu,\mu)})^H, \sum_{\mu=1}^{N_t} [\mathbf{B}_i]_\mu^T \otimes (\bar{\mathbf{H}}^{(\nu,\mu)} \mathbf{P}_2)]$, $\forall i \in [0, N_s-1]$, and \mathbf{P}_2 is an $(N_{od}+Q) \times (N_{od}+Q)$ time reversal matrix. Similar to A5) and A5'), we need the following assumption.

A5'') Channels $\bar{\mathbf{H}}^{(\nu,\mu)}$ are coprime, i.e., $\det \left(\sum_{\nu=1}^{N_r} \sum_{\mu=1}^{N_t} \bar{\mathbf{H}}^{(\nu,\mu)} (\bar{\mathbf{H}}^{(\nu,\mu)})^* \right) \neq 0$.

The output of the MRC combiner in (34) is

$$\mathbf{z}_i = \frac{1}{\sqrt{N_t}} \left(\sum_{\nu=1}^{N_r} \sum_{\mu=1}^{N_t} \bar{\mathbf{H}}^{(\nu,\mu)} (\bar{\mathbf{H}}^{(\nu,\mu)})^H \right)^{1/2} \mathbf{T}_{zp} \mathbf{s}_i + \boldsymbol{\xi}_i.$$

To decode \mathbf{s}_i from \mathbf{z}_i , $\mathcal{G}(\cdot)$ can again rely on sphere-decoding implemented on blocks of size N_{od} .

Similar to the CP-based scheme, the ZP-based one also enables maximum diversity. When $r_h = N_t N_r (Q+1)$, we find the coding gain as (see Appendix D for a proof).

$$G_c = (\det(\mathbf{R}_h))^{1/r_h} \frac{d_{\min}^2}{N_t}. \quad (35)$$

The coding and decoding processes for the ZP-based scheme are summarized in Fig. 4, and the major results on performance are established by the following proposition:

Proposition 4: ZP-based STDO block codes enable the maximum space-Doppler diversity $G_d = r_h, \forall N_{od} > 0$. When the channel correlation matrix \mathbf{R}_h has full rank $N_t N_r (Q+1)$, the ZP-based design achieves the maximum coding gain G_c^{\max} of linearly coded systems. The transmission rate of ZP-based design is $r_{\text{stbc}} N_{od} / (N_{od} + Q)$, where r_{stbc} is the rate of the corresponding block ST codes (specified in [20]).

Remark 2: Comparing our three STDO designs, we note that i) all schemes guarantee the maximum diversity gain; ii) DPS and ZP-based schemes achieve also the maximum coding gain, while the CP-based scheme achieves the maximum coding gain asymptotically (as N_{od} increases); iii) to guarantee the maximum diversity gain, the CP-based scheme provides the lowest decoding complexity; iv) to deal with IBI, CP- and ZP-based approaches rely on CP or ZP guards, which consume extra bandwidth compared with the DPS scheme that does not require any guard. Furthermore, together with the GCOD design benefits [19], our CP- and ZP-based STDO codecs inherit also its limitation in suffering up to 50% rate loss when $N_t > 2$ antennas are signaling with complex constellations. Notwithstanding, the DPS attains full rate for any N_t .

VI. SIMULATED PERFORMANCE

We present simulations to confirm the performance of our maximum diversity schemes.

Test Case 1 (Comparisons Among the Three STDO Codecs): We compare DPS, CP-Based, and ZP-Based schemes with $N_t = 2$ transmit antennas, $Q+1 = 3$ bases per channel, and BEM parameters that are i.i.d., Gaussian, with mean zero, and variance $1/(Q+1)$. We choose quadrature phase shift keying (QPSK) modulation for all these schemes. The number of information symbols per block is $P = K = 24$. For DPS, the transmitted block length $N = 24$, while for CP- and ZP-based schemes, the block length $N = 28$ because of the CP and ZP guards, respectively. The linear precoder with grouping is employed for DPS and CP-based schemes with group sizes $N_{\text{sub}} = 6$ and $\bar{N}_{\text{sub}} = 3$, respectively. Fig. 5 depicts the BER performance of these three codecs. SD has been employed

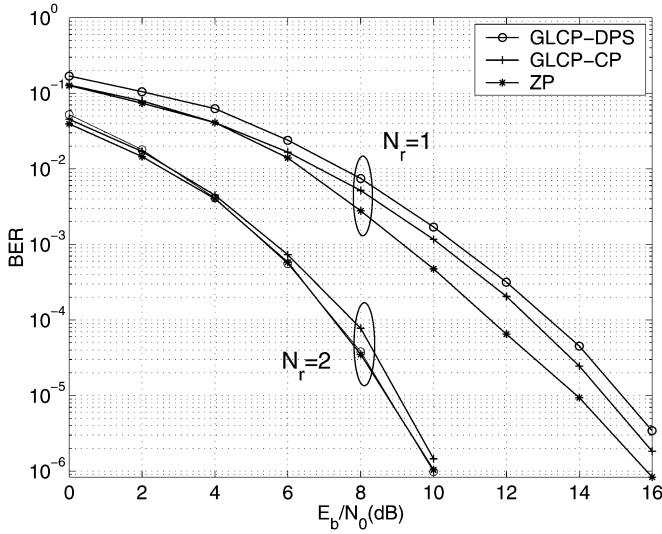
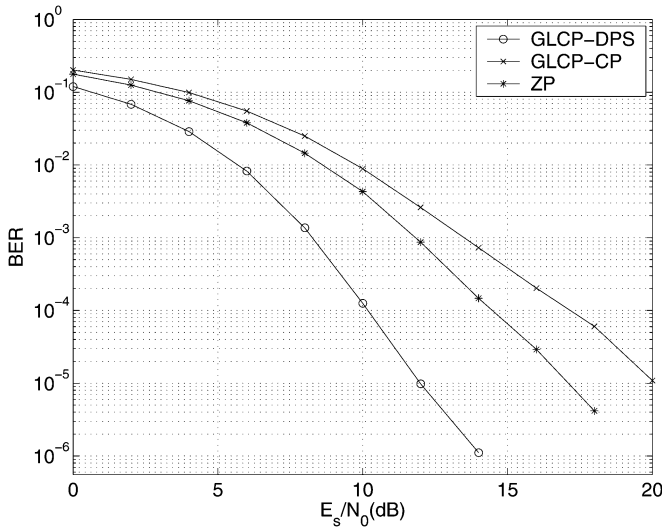


Fig. 5. Comparisons among the three proposed STDO codecs.

Fig. 6. Comparisons among the three proposed STDO codecs when $N_t = 4$.

for all schemes. We observe that i) from the slope of the BER curves for $N_r = 1$, all three schemes guarantee the maximum diversity order $G_d^{\max} = N_t(Q + 1) = 6$; ii) with either $N_r = 1$ or 2, the ZP-based scheme exhibits the best performance among the three; iii) compared with CP, the performance of DPS incurs about 0.5 dB loss at high SNR for $N_r = 1$; iv) as N_r increases, the performance difference among three schemes diminishes at high SNR.

Fig. 6 depicts the performance of our three STDO when $N_t = 4$. For CP- and ZP-based schemes, we select the block ST code as in [20, Eq. (38)], which loses 50% rate. To maintain similar rates, we select QPSK for CP- and ZP-based schemes and binary phase shift keying (BPSK) for DPS with the same symbol power. The information block length is $K = 36$. From Fig. 6, we observe that DPS outperforms both CP and ZP. Note that even in this case, CP- and ZP-based schemes have lower rate [(9/11) bit/sec/Hz] than DPS (1 bit/sec/Hz).

Test Case 2 (Comparisons With [19]): In this example, we compare our DPS scheme with the smart-greedy code proposed

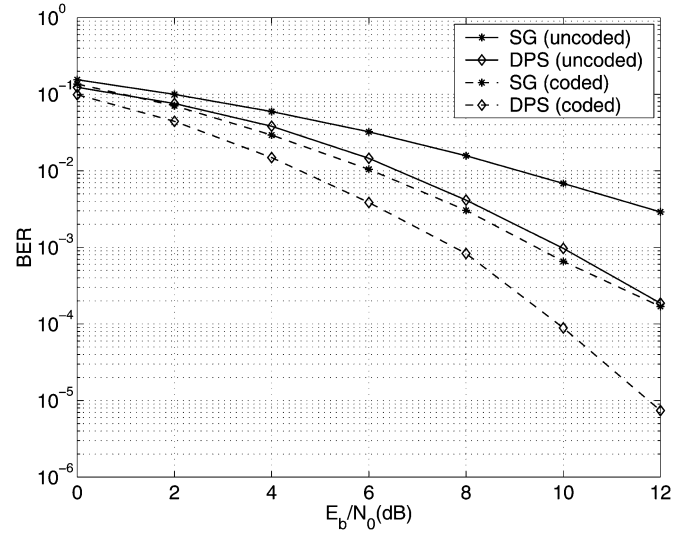


Fig. 7. Comparison of DPS with the smart-greedy (SG) codes in [19].

in [19] for $(N_t, N_r) = (2, 1)$. To maintain the same rate, we select BPSK for our DPS scheme and use the code in [19, Ex. 3.9.2]. Each channel has $Q + 1 = 3$ bases, and the channel coefficients are i.i.d. with mean zero and variance $1/(Q + 1)$. First, we consider the uncoded setup. The information block length is $K = P = 30$. The number of groups for DPS is $N_g = 5$ so that these two schemes have comparable decoding complexity. Fig. 7 depicts the BER versus SNR comparison for the smart-greedy code and our DPS (the solid lines). It is evident that DPS outperforms the “smart-greedy” coding because the former guarantees the full space-Doppler diversity.

Furthermore, we consider the coded case for both schemes. We select a (7,3) Reed–Solomon coder with block interleaving. The number of information bits is 90. Therefore, the length of the coded block of bits is 210. We select the depth of the block interleaver as 42. For the DPS design, we split the coded bits into five blocks. Each block is divided into seven groups. The simulation results are shown in Fig. 7 (the dashed lines). Note that the DPS scheme still outperforms the smart-greedy codes remarkably.

Test Case 3 (Correlated Channels): In this example, we investigate the performance of our three schemes when the channel coefficients are not i.i.d. The carrier frequency is now $f_0 = 2$ GHz, and the maximum mobile speed is $v_{\max} = 160$ km/hr. For these f_0 and v_{\max} values, we find that $f_{\max} \approx 296.3$ Hz. The sampling period is defined as $T_s = 0.15$ ms. Thus, the number of bases is $Q = 4$. We generate each channel correlation matrix $E[\mathbf{h}^{(\nu,\mu)}(\mathbf{h}^{(\nu,\mu)})^H] = \mathbf{U}\mathbf{\Lambda}$, where \mathbf{U} is a $(Q + 1) \times (Q_{\text{real}} + 1)$ unitary matrix, and $\mathbf{\Lambda}$ is a $(Q_{\text{real}} + 1) \times (Q_{\text{real}} + 1)$ diagonal matrix. The i th entry of $\mathbf{\Lambda}$ is $[\mathbf{\Lambda}]_{i,i} = \gamma \left(\pi \sqrt{f_{\max}^2 - ((i - 2Q_{\text{real}})/(KT_s))^2} \right)^{-1}$, where γ is a normalizing factor. It is clear that the choice of entries of $\mathbf{\Lambda}$ reflects the underlying Doppler spectrum. We consider the channels corresponding to different antennas to be independent. Then, we generate $\mathbf{h}^{(\nu,\mu)} = \mathbf{U}\mathbf{\Lambda}\bar{\mathbf{h}}^{(\nu,\mu)}$, where the entries of $\bar{\mathbf{H}}^{(\nu,\mu)}$ are i.i.d. with zero mean and unit variance. We consider $N_t = 2$ and $N_r = 1$ for all schemes. In this example, $Q_{\text{real}} = 2$. For the CP-based scheme, we still use the

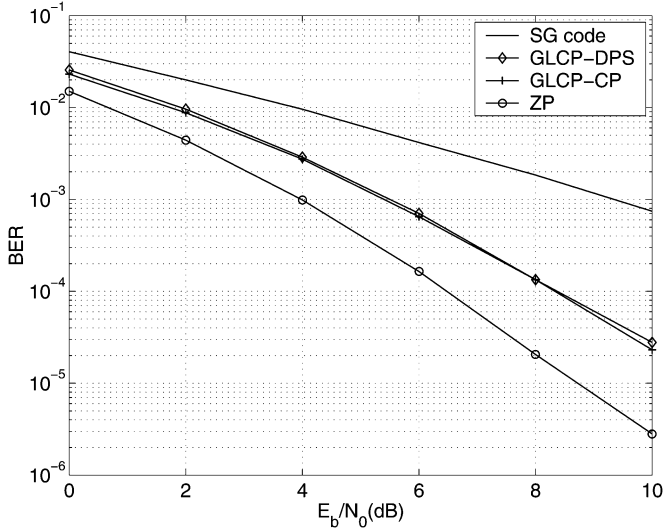


Fig. 8. Comparisons among three proposed schemes and the smart-greedy (SG) code in [19], with correlated channels.

GLCP method with group size $\bar{N}_{\text{sub}} = 3$, whereas for the DPS method, we select $N_{\text{sub}} = 6$. The information block length for all schemes is $K = 36$. Hence, for CP- and ZP-based schemes, the transmitted block length is $N = 44$. We select BPSK modulation throughout this experiment. The rate for DPS and the smart-greedy code of [19] is 1 bit/sec/Hz, whereas the rate is (9/11) bits/sec/Hz for CP- and ZP-based schemes.

Fig. 8 depicts the BER performance for our three proposed schemes and the smart-greedy code in [19, Ex. 3.9.2]. It can be seen that all our proposed schemes achieve full diversity (in this case, it is $G_d = 6$) and outperform the “smart-greedy” code of [19]. Compared with the CP-based and DPS schemes, the ZP-based scheme has about 1 dB gain at $\text{BER} = 10^{-4}$. However, note that both CP- and ZP-based schemes have lower rate than DPS.

Test Case 4 (Channels Generated by Jakes’ Model): For the single-antenna case, we have shown that even for channels generated by Jakes’ model, our Doppler diversity claim holds true [15]. In this example, we will test the performance of our three STDO schemes when channels are generated by the Jakes’ model [10] but are spatially independent. The parameters for Jakes’ model are carrier frequency $f_0 = 5.2$ GHz, mobile speed $v_{\text{max}} = 96$ km/hr, and sampling period $T_s = 7 \mu\text{s}$. The transmitted block length is $N = 300$ for DPS and 304 for ZP- and CP-based schemes. The BER performance of the schemes with $(N_t, N_r) = (2, 1)$ is depicted in Fig. 9. In the same figure, we plot the single-antenna case when GLCP is used to enable Doppler diversity. From the simulation results, we observe that ZP- and CP-based schemes exhibit error floor because i) after FFT and IFFT operations, the circulant matrix 24 is full (the generating vector has length N instead of $Q + 1$, although the number of dominant entries is only $Q + 1$), and ii) after CP or ZP insertion, the equivalent channel matrices [cf. (29)] is not exactly block-diagonal, which is due to the presence of inter-subblock interference. Note that at the receiver, we still rely on MRC as Section V in order to retain the low decoding complexity of the ZP- and CP-based methods. This explains

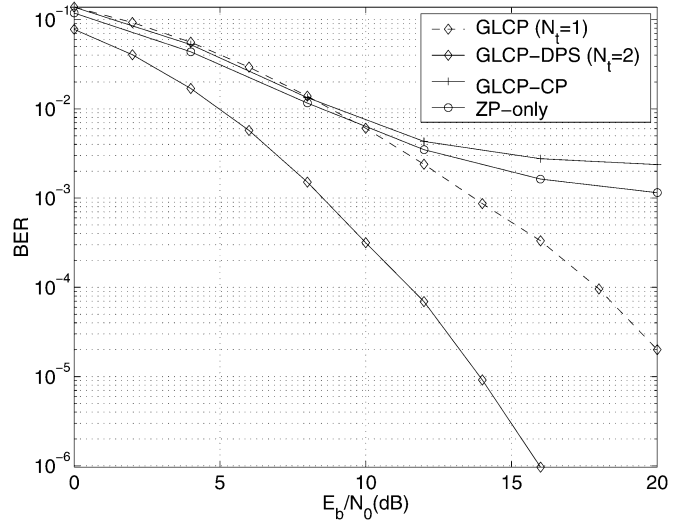


Fig. 9. Comparisons among three proposed schemes with channels generated by Jakes’ model.

why the performance of these two schemes shows an error floor at high SNR. On the other hand, GLCP-DPS scheme enjoys joint Doppler and spatial diversity. Comparing with the single antenna case, we deduce that GLCP-DPS enables the joint space-Doppler diversity, even when the channels are generated the Jakes’ model and, thus, do not exactly adhere to the BEM.

VII. CONCLUDING SUMMARY

We relied on an existing basis expansion model (BEM) to benchmark the performance of multiantenna space-time coded transmissions over correlated time-selective fading MIMO channels. Specifically, we expressed in closed form the maximum achievable space-Doppler diversity gain in terms of the number of transmit-receive antennae and the number of bases. Furthermore, we quantified in closed-form the maximum possible coding gain for all linearly coded space-time transmissions and found it to depend on the rank of the BEM coefficients’ correlation matrix and the minimum Euclidean distance of the constellation used.

In addition to performance limits, the BEM enabled us to develop space-time-Doppler (STDO) coded designs capable of achieving (or approaching) these gains, using only knowledge of the maximum Doppler spread. We established two neat BEM properties that played an instrumental role in these designs: i) Multiple (N_t) BEMs with $Q + 1$ bases each can be rendered mathematically equivalent to a single faster BEM with $N_t(Q + 1)$ bases, via a digital phase sweeping operation at the transmitters; and ii) a BEM for time-selective channels is dual to a tapped delay line model for frequency-selective channels, which allows designs developed for one model to be used for the other after incorporating appropriate FFT-based operations at the transmit-receive sides.

The first property led us to an STDO-coded system based on a novel digital phase sweeping design, which collects the maximum joint space-Doppler diversity and large coding gains, whereas it facilitates application of SISO channel estimators and affords a low-complexity modular implementation when

working with linearly precoded small-size groups of symbols. Its unique feature is full rate (1 symbol/sec/Hz) operation, regardless of the constellation and the number of transmit-receive antennae. The second property showed us the way to adjust existing space-time coded designs maximizing space-multipath diversity over frequency-selective channels to collect joint space-Doppler gains over our time-selective MIMO channel. Using the same property in the reverse direction, we established that the limits on coding gains we derived for the BEM apply to space-time coded transmissions over frequency-selective MIMO channels as well. The multipath-inspired designs yielded space-time-Doppler coded block transmissions with cyclic prefix or zero padding guard intervals. The former system affords the lowest (FFT-based) complexity, whereas the latter exhibits the best performance. With two transmit-antennas, they have full rate, but with more transmit-antennas, they both suffer the same rate loss as space-time block orthogonal designs do with complex constellations.

All three designs were developed in a unifying framework that entails three-stages (outer-middle-inner) of encoding and decoding. Their relative strengths were delineated both analytically and with simulations that also compared them with an existing system. Both coded and uncoded transmissions were tested over i.i.d. and correlated channels and confirmed that the proposed designs outperform existing alternatives as they exploit fully the joint space-Doppler diversity that becomes available with time-selective channels.

APPENDIX A PROOF OF (13)

Let $d^2(\tilde{\mathbf{x}}, \tilde{\mathbf{x}}') = \mathbf{h}^H \mathbf{A}_e \mathbf{h}$, where

$$\begin{aligned} \mathbf{h} &:= \left[h_0^{(1,1)}, \dots, h_Q^{(1,1)}, \dots, h_Q^{(N_r, N_t)} \right]^T \\ &\quad N_r N_t (Q+1) \times 1 \\ \mathbf{A}_e &:= \mathbf{I}_{N_r} \otimes (\mathbf{E}_e^H \mathbf{E}_e), N_r N_t (Q+1) \times N_r N_t (Q+1) \\ \mathbf{E}_e &:= [D_e^{(1)} \boldsymbol{\Omega}, \dots, D_e^{(N_t)} \boldsymbol{\Omega}], N \times N_t (Q+1) \\ \boldsymbol{\Omega} &:= [\boldsymbol{\omega}_0, \dots, \boldsymbol{\omega}_Q], N \times (Q+1) \\ \boldsymbol{\omega}_q &:= [1, \exp(j\omega_q), \dots, \exp(j\omega_q(N-1))]^T. \end{aligned} \quad (36)$$

Suppose temporarily that $G_d^{\max} = r_h$ in (10) has been achieved, i.e., that $\boldsymbol{\Psi}_e$ has full rank $\forall \mathbf{e} \neq \mathbf{0}$. Furthermore, using the definition of \mathbf{A}_e in (36), when $r_h = N_r N_t (Q+1)$, we find that

$$\begin{aligned} \det(\mathbf{A}_e) &= (\det(\mathbf{E}_e^H \mathbf{E}_e))^{N_r}, \quad \text{with} \\ \mathbf{E}_e^H \mathbf{E}_e &= \begin{bmatrix} \mathbf{E}_e^{(1)} & \diamond & \dots & \diamond \\ \diamond & \mathbf{E}_e^{(2)} & \dots & \diamond \\ \vdots & \vdots & \ddots & \vdots \\ \diamond & \diamond & \diamond & \mathbf{E}_e^{(N_t)} \end{bmatrix} \\ \mathbf{E}_e^{(\mu)} &:= \begin{bmatrix} \|\mathbf{e}_\mu\|^2 & \diamond & \diamond \\ \diamond & \|\mathbf{e}_\mu\|^2 & \diamond \\ \vdots & \ddots & \vdots \\ \diamond & \diamond & \|\mathbf{e}_\mu\|^2 \end{bmatrix}_{(Q+1) \times (Q+1)} \end{aligned}$$

where \diamond stands for terms that are irrelevant at this point, and $\mathbf{e}_\mu := \mathbf{v}_\mu - \mathbf{v}'_\mu$. Based on (7), we find G_c in (9) as

$$\begin{aligned} G_c &= \min_{\forall \mathbf{e} \neq \mathbf{0}} [\det(\boldsymbol{\Psi}_e)]^{1/r_h} \\ &= \min_{\forall \mathbf{e} \neq \mathbf{0}} [\det(\boldsymbol{\Lambda}_h) \det(\mathbf{A}_e)]^{1/r_h}. \end{aligned} \quad (37)$$

Starting from (5), given $\mathbf{e}_\mu := \mathbf{v}_\mu - \mathbf{v}'_\mu$, we can upper-bound G_c in (37) as [cf. Hadamard's inequality [9, p. 117]]

$$G_c \leq (\det(\mathbf{R}_h))^{1/r_h} \min_{\forall \mathbf{e} \neq \mathbf{0}} \left(\prod_{\mu=1}^{N_t} \|\mathbf{e}_\mu\|^2 \right)^{1/N_t}. \quad (38)$$

Based on (12), the equipowered condition in (11) is equivalent to

$$\sum_{p=0}^{P-1} \left(\mathbf{a}_p^{(\mu)} \right)^H \mathbf{a}_p^{(\mu)} + \left(\mathbf{b}_p^{(\mu)} \right)^H \mathbf{b}_p^{(\mu)} = \frac{P}{N_t}, \quad \forall \mu \in [1, N_t]. \quad (39)$$

Arguing by contradiction, it follows readily from (39) that

$$\min_{\forall n \in [0, N-1]} \left(\sum_{p=0}^{P-1} \left(\left| [\mathbf{a}_p^{(\mu)}]_n \right|^2 + \left| [\mathbf{b}_p^{(\mu)}]_n \right|^2 \right) \right) \leq \frac{1}{N_t}. \quad (40)$$

Now, let $\mathcal{A}_v^{(\mu)}$ be the finite alphabet set for the entries of \mathbf{V}_μ . Notice that the left-hand side of (40) is related to the minimum Euclidean distance $\delta_{\min}^{(\mu)}$ among the constellation points in $\mathcal{A}_v^{(\mu)}$. If we let d_{\min} denote the same distance for the points in \mathcal{A}_s , we deduce that

$$\begin{aligned} \left(\delta_{\min}^{(\mu)} \right)^2 &= \min_{v, v' \in \mathcal{A}_v^{(\mu)}} |v - v'|^2 \\ &\leq d_{\min}^2 \min_{\forall n \in [0, N-1]} \left(\sum_{p=0}^{P-1} \left(\left| [\mathbf{a}_p^{(\mu)}]_n \right|^2 + \left| [\mathbf{b}_p^{(\mu)}]_n \right|^2 \right) \right) \\ &\leq \frac{d_{\min}^2}{N_t}, \quad \forall \mu \in [1, N_t]. \end{aligned} \quad (41)$$

Based on (41), we further upper-bound the coding gain in (38) for our linearly coded system by

$$G_c^{\max} = (\det(\mathbf{R}_h))^{1/r_h} \frac{d_{\min}^2}{N_t}.$$

Note that the maximum coding gain G_c^{\max} depends on the underlying constellation through d_{\min}^2 and is inversely proportional to the number of transmit antennas N_t because of the power splitting.

APPENDIX B PROOF OF PROPOSITION 2

To derive the diversity and coding gains of our DPS design, we need to find the Euclidean distance between \mathbf{z}_g and \mathbf{z}'_g , corresponding to two different symbol blocks \mathbf{s}_g and \mathbf{s}'_g . From

(23), we have $d^2(\mathbf{z}_g, \mathbf{z}'_g) = \sum_{i=1}^{N_r} \|\mathbf{D}_{e,g} \boldsymbol{\Omega}_g \mathbf{h}^{(\nu)}\|^2$, where $\mathbf{h}^{(\nu)} := [h_0^{(\nu)}, \dots, h_{N_t(Q+1)-1}^{(\nu)}]^T$, $\boldsymbol{\Omega}_g := [\boldsymbol{\omega}_0, \dots, \boldsymbol{\omega}_{N_t(Q+1)-1}]$, and $\mathbf{\Omega}_g := [\exp(j\omega_q g), \exp(j\omega_q(N_g + g)), \dots, \exp(j\omega_q(N_g(N_{\text{sub}} - 1) + g))]^T$, and $\mathbf{D}_{e,g} = \text{diag}[\boldsymbol{\Theta}_{\text{sub}}(\mathbf{s}_g - \mathbf{s}'_g)]/\sqrt{N_t}$. The diversity order is the rank of the matrix

$$\boldsymbol{\Psi}_e = (\mathbf{U}_h \boldsymbol{\Lambda}_h^{1/2})^{\mathcal{H}} (\mathbf{I}_{N_r} \otimes (\boldsymbol{\Omega}_g^{\mathcal{H}} \mathbf{D}_{e,g}^* \mathbf{D}_{e,g} \boldsymbol{\Omega}_g)) \mathbf{U}_h \boldsymbol{\Lambda}_h^{1/2}.$$

According to [23], there always exists a linear precoder $\boldsymbol{\Theta}_{\text{sub}}$ that guarantees the full rank of $\mathbf{D}_{e,g}$, when $\mathbf{s}_g \neq \mathbf{s}'_g$. The matrix $\boldsymbol{\Omega}_g$ has full rank. If $N_{\text{sub}} \geq N_t(Q+1)$, then arguing as in Section III, we infer that DPS achieves the maximum diversity order $G_d = r_h$. The coding gain is $G_c = \min_{\mathbf{e} \neq \mathbf{0}} [\det(\boldsymbol{\Psi}_e)]^{1/r_h}$.

Furthermore, when $r_h = N_r N_t(Q+1)$ and $N_{\text{sub}} = N_t(Q+1)$, based on the equi-spaced grouping design, we can verify that $\boldsymbol{\Omega}_g \boldsymbol{\Omega}_g^{\mathcal{H}} = \boldsymbol{\Omega}_g^{\mathcal{H}} \boldsymbol{\Omega}_g = N_{\text{sub}} \mathbf{I}_{N_{\text{sub}}}$. Therefore, the coding gain is

$$G_c = (\det(\mathbf{R}_h))^{1/r_h} N_{\text{sub}} \min_{\mathbf{e} \neq \mathbf{0}} (\det(\mathbf{D}_{e,g}^* \mathbf{D}_{e,g}))^{1/N_{\text{sub}}}. \quad (42)$$

Equation (42) shows that the maximum coding gain depends on $\mathbf{D}_{e,g}$ and, thus, on the design of $\boldsymbol{\Theta}_{\text{sub}}$. For designing the latter, we borrow the following result from [23].

Result 1 [23, Prop. 5]: Consider a quadrature amplitude modulation (QAM) [or pulse amplitude modulation (PAM)] constellation \mathcal{A}_s with minimum distance d_{\min} . For $N_{\text{sub}} \in \mathbb{N}$, the linear precoder $\boldsymbol{\Theta}_{\text{sub}}$ in (17) can be designed such that

$$\begin{aligned} (\ln 2) \left(\frac{d_{\min}^2}{N_{\text{sub}} N_t} \right) &\leq \min_{\mathbf{e} \neq \mathbf{0}} (\det(\mathbf{D}_{e,g}^* \mathbf{D}_{e,g}))^{1/N_{\text{sub}}} \\ &\leq \frac{d_{\min}^2}{N_{\text{sub}} N_t} \end{aligned} \quad (43)$$

when the number N_{sub} satisfies a certain algebraic property, the upper bound in (43) is achieved. Based on Result 1 and the unilarity of $\boldsymbol{\Omega}_g$ [since we choose $N_{\text{sub}} = n_t(q+1)$], we have

$$\begin{aligned} (\ln 2) (\det(\mathbf{R}_h))^{1/r_h} \frac{d_{\min}^2}{N_t} &\leq G_c \\ &\leq (\det(\mathbf{R}_h))^{1/r_h} \frac{d_{\min}^2}{N_t}. \end{aligned} \quad (44)$$

Notice that even the lower bound is about 70% of the upper bound. This result implies that when our grouped DPS design utilizes the linear precoder of [23], it can achieve the maximum coding gain

$$G_c^{\max} = (\det(\mathbf{R}_h))^{1/r_h} \frac{d_{\min}^2}{N_t}.$$

Checking with (12), we confirm that our DPS design is a linearly coded ST system. Recalling that the maximum diversity and coding gains of the latter are given by (10) and (13), we have shown that our GLPC-based DPS scheme achieves G_d^{\max} and G_c^{\max} .

APPENDIX C PROOF OF PROPOSITION 3

To derive the diversity and coding gains for the CP-based ST block STDO, we calculate the Euclidean distance of $\mathbf{z}_{i,g}$ and $\mathbf{z}'_{i,g}$ as

$$d^2(\mathbf{z}_{i,g}, \mathbf{z}'_{i,g}) = \frac{\rho^2}{N_t} \sum_{\nu=1}^{N_r} \sum_{\mu=1}^{N_t} \|\mathbf{D}_{e,g} \boldsymbol{\Omega}_g \mathbf{h}^{(\nu,\mu)}\|^2$$

where $\boldsymbol{\Omega}_g$ is the corresponding rows from $\boldsymbol{\Omega}$ in (36) for the g group $\mathbf{h}^{(\nu,\mu)} := [h_0^{(\nu,\mu)}, \dots, h_Q^{(\nu,\mu)}]^T$, and $\mathbf{D}_{e,g} = \text{diag}[\boldsymbol{\Theta}_{\text{sub}}(\mathbf{s}_g - \mathbf{s}'_g)]/\sqrt{N_t}$. Similar to the DPS design, $\boldsymbol{\Theta}_{\text{sub}}$ guarantees the full rank of $\mathbf{D}_{e,g}$ for any $\mathbf{s}_g \neq \mathbf{s}'_g$. Therefore, it follows readily that when $N_{\text{sub}} \geq Q+1$, the maximum diversity order r_h is achieved.

Based on (12), we can verify that our CP-based approach constitutes also a linearly coded transmission. Similar to the DPS design, when $r_h = N_r N_t(Q+1)$, and we select $N_{\text{sub}} = Q+1$, the coding gain for this CP-based scheme satisfies (31) [cf. (13)].

APPENDIX D PROOF OF (35)

We express the Euclidean distance between \mathbf{z}_i and \mathbf{z}'_i as

$$d^2(\mathbf{z}_i, \mathbf{z}'_i) = \frac{1}{N_t} \sum_{\nu=1}^{N_r} \sum_{\mu=1}^{N_t} \|\mathbf{E}_i \mathbf{h}^{(\nu,\mu)}\|^2 \quad (45)$$

where \mathbf{E}_i is a Toeplitz matrix generated by $\mathbf{e}_i = \mathbf{s}_i - \mathbf{s}'_i$. When \mathbf{R}_h has full rank $r_h = N_r N_t(Q+1)$, the coding gain of the ZP-based scheme becomes [cf. (37) and (45)]

$$G_c = \frac{1}{N_t} (\det(\mathbf{R}_h))^{1/r_h} \min_{\mathbf{e}_i \neq \mathbf{0}} [\det(\mathbf{E}_i^{\mathcal{H}} \mathbf{E}_i)]^{1/Q+1} \quad (46)$$

where \mathbf{E}_i is an $(N_{\text{sub}} + Q) \times (Q+1)$ Toeplitz matrix with first column $[\mathbf{e}_i^T \mathbf{0}^T]^T$. Considering single-error events, i.e. $\mathbf{e}_i = [\mathbf{0}_{m-1} \ \mathbf{e} \ \mathbf{0}_{N_{\text{sub}}-m}]^T$, $\forall m \in [1, N_{\text{sub}}]$, with $\mathbf{e} := \mathbf{s} - \mathbf{s}'$, we obtain

$$[\det(\mathbf{E}_i^{\mathcal{H}} \mathbf{E}_i)]^{1/Q+1} = |\mathbf{e}|^2 \geq d_{\min}^2.$$

Recalling (46), we can upper bound the coding gain as

$$G_c \leq (\det(\mathbf{R}_h))^{1/r_h} \frac{d_{\min}^2}{N_t}. \quad (47)$$

To show that the ZP-based approach achieves this upper bound of the coding gain, we need to show that $\det(\mathbf{E}_i^{\mathcal{H}} \mathbf{E}_i) \geq d_{\min}^{2(Q+1)}$, $\forall \mathbf{e}_i \neq \mathbf{0}$.

Suppose the first nonzero entry of the error vector \mathbf{e}_i is the m th, and split the matrix \mathbf{E}_i into two submatrices $\mathbf{E}_{i,1}$ and $\mathbf{E}_{i,2}$, where $\mathbf{E}_{i,1}$ contains the first $m+Q$ rows of \mathbf{E}_i , and $\mathbf{E}_{i,2}$ includes the remaining rows. Since $\mathbf{E}_i = [\mathbf{E}_{i,1}^T, \mathbf{E}_{i,2}^T]^T$,

we obtain $\det(\mathbf{E}_i^H \mathbf{E}_i) = \det(\mathbf{E}_{i,1}^H \mathbf{E}_{i,1} + \mathbf{E}_{i,2}^H \mathbf{E}_{i,2})$, and as the matrix $\mathbf{E}_{i,1}^H \mathbf{E}_{i,1}$ is positive definite, we have

$$\begin{aligned} \det(\mathbf{E}_i^H \mathbf{E}_i) &= \det(\mathbf{E}_{i,1}^H \mathbf{E}_{i,1}) \det(\mathbf{I}_{Q+1} + (\mathbf{E}_{i,1}^H \mathbf{E}_{i,1})^{-1} \mathbf{E}_{i,2}^H \mathbf{E}_{i,2}). \end{aligned}$$

Because $\mathbf{E}_{i,2}^H \mathbf{E}_{i,2}$ is positive semi-definite, the matrix $(\mathbf{E}_{i,1}^H \mathbf{E}_{i,1})^{-1} \mathbf{E}_{i,2}^H \mathbf{E}_{i,2}$ is positive semi-definite as well. Hence, we find that

$$\begin{aligned} \det(\mathbf{I}_{Q+1} + (\mathbf{E}_{i,1}^H \mathbf{E}_{i,1})^{-1} \mathbf{E}_{i,2}^H \mathbf{E}_{i,2}) &= \det(\mathbf{I}_{Q+1} + \mathbf{\Lambda}_E) \geq 1 \end{aligned}$$

where $\mathbf{\Lambda}_E = \text{diag}[\lambda_{E,0}, \dots, \lambda_{E,Q}]$, and $\lambda_{E,q}$'s are the eigenvalues of $(\mathbf{E}_{i,1}^H \mathbf{E}_{i,1})^{-1} \mathbf{E}_{i,2}^H \mathbf{E}_{i,2}$, which are non-negative. From our design of $\mathbf{E}_{i,1}$, it is easy to see that $\det(\mathbf{E}_{i,1}^H \mathbf{E}_{i,1}) = |e|^{2(Q+1)} \geq d_{\min}^{2(Q+1)}$. Therefore, we obtain

$$\det(\mathbf{E}_i^H \mathbf{E}_i) \geq d_{\min}^{2(Q+1)}, \quad \forall \mathbf{e}_i \neq \mathbf{0}.$$

Hence, the coding gain of the ZP-based scheme is lower bounded by

$$G_c \geq (\det(\mathbf{R}_h))^{1/r_h} \frac{d_{\min}^2}{N_t}. \quad (48)$$

Combining (47) and (48), we have proved (35).

REFERENCES

- [1] S. L. Ariyavisitakul, "Turbo space-time processing to improve wireless channel capacity," *IEEE Trans. Commun.*, vol. 48, no. 8, pp. 1347–1359, Aug. 2000.
- [2] H. Bölcskei and A. J. Paulraj, "Space-frequency codes for broadband fading channels," in *Proc. Wireless Commun. Networking Conf.*, vol. 1, Chicago, IL, Sep. 23–28, 2000, pp. 1–6.
- [3] J. K. Cavers, "An analysis of pilot symbol assisted modulation for Rayleigh fading channels," *IEEE Trans. Veh. Technol.*, vol. 40, no. 4, pp. 686–693, Nov. 1991.
- [4] G. J. Foschini and M. J. Gans, "On limits of wireless communication in a fading environment when using multiple antennas," *Wireless Pers. Commun.*, vol. 6, no. 3, pp. 311–335, Mar. 1998.
- [5] G. B. Giannakis and C. Tepedelenlioglu, "Basis expansion models and diversity techniques for blind identification and equalization of time-varying channels," *Proc. IEEE*, vol. 86, pp. 1969–1986, Nov. 1998.
- [6] G. H. Golub and C. F. van Loan, *Matrix Computations*, Third ed. Baltimore, MD: Johns Hopkins Univ. Press, 1996.
- [7] B. Hassibi and B. M. Hochwald, "High-rate codes that are linear in space and time," *IEEE Trans. Inf. Theory*, vol. 48, no. 7, pp. 1804–1824, Jul. 2002.
- [8] A. Hiroike, F. Adachi, and N. Nakajima, "Combined effects of phase sweeping transmitter diversity and channel coding," *IEEE Trans. Veh. Technol.*, vol. 41, no. 2, pp. 170–176, May 1992.
- [9] R. A. Horn and C. R. Johnson, *Topics in Matrix Analysis*. Cambridge, U.K.: Cambridge Univ. Press, 1991.
- [10] W. C. Jakes, *Microwave Mobile Communications*. New York: Wiley, 1974.
- [11] W.-Y. Kuo and M. P. Fitz, "Design and analysis of transmitter diversity using intentional frequency offset for wireless communications," *IEEE Trans. Veh. Technol.*, vol. 46, no. 4, pp. 871–881, Nov. 1997.
- [12] Z. Liu, Y. Xin, and G. B. Giannakis, "Linear constellation precoding for OFDM with maximum multipath diversity and coding gains," *IEEE Trans. Commun.*, vol. 51, no. 3, pp. 416–427, Mar. 2003.
- [13] —, "Space-time-frequency coded OFDM over frequency-selective fading channels," *IEEE Trans. Signal Process.*, vol. 50, no. 10, pp. 2465–2476, Oct. 2002.
- [14] B. Lu and X. Wang, "Space-time code design in OFDM systems," in *Proc. Global Telecommun. Conf.*, vol. 2, San Francisco, CA, Nov.–Dec. 27–1, 2000, pp. 1000–1004.
- [15] X. Ma and G. B. Giannakis, "Maximum-diversity transmissions over doubly-selective wireless channels," *IEEE Trans. Inf. Theory*, vol. 49, no. 7, pp. 1832–1840, Jul. 2003.
- [16] A. Narula, M. D. Trott, and G. W. Wornell, "Performance limits of coded diversity methods for transmitter antenna arrays," *IEEE Trans. Inf. Theory*, vol. 45, no. 7, pp. 2418–2433, Nov. 1999.
- [17] J. G. Proakis, *Digital Communications*, Fourth ed: McGraw-Hill, 2001.
- [18] N. Seshadri and J. H. Winters, "Two signaling schemes for improving the error performance of frequency-division duplex (FDD) transmission systems using transmitter antenna diversity," *Int. J. Wireless Inf. Networks*, pp. 49–60, 1994.
- [19] V. Tarokh, N. Seshadri, and A. R. Calderbank, "Space-time codes for high data rate wireless communication: Performance criterion and code construction," *IEEE Trans. Inf. Theory*, vol. 44, no. 3, pp. 744–765, Mar. 1998.
- [20] V. Tarokh, H. Jafarkhani, and A. R. Calderbank, "Space-time block codes from orthogonal designs," *IEEE Trans. Inf. Theory*, vol. 45, no. 5, pp. 1456–1467, Jul. 1999.
- [21] E. Viterbo and J. Boutros, "A universal lattice code decoder for fading channels," *IEEE Trans. Inf. Theory*, vol. 45, no. 5, pp. 1639–1642, Jul. 1999.
- [22] Z. Wang and G. B. Giannakis, "Complex-field coding for OFDM over fading wireless channels," *IEEE Trans. Inf. Theory*, vol. 49, no. 3, pp. 707–720, Mar. 2003.
- [23] Y. Xin, Z. Wang, and G. B. Giannakis, "Space-time diversity systems based on linear constellation precoding," *IEEE Trans. Wireless Commun.*, vol. 2, no. 2, pp. 294–309, Mar. 2003.
- [24] Q. Yan and R. S. Blum, "Robust space-time block coding for rapid fading channels," in *Proc. IEEE Global Telecommun. Conf.*, vol. 1, San Antonio, TX, Nov. 25–29, 2001, pp. 460–464.
- [25] S. Zhou and G. B. Giannakis, "Space-time coding with maximum diversity gains over frequency-selective fading channels," *IEEE Signal Process. Lett.*, vol. 8, pp. 269–272, Oct. 2001.
- [26] —, "Single-carrier space-time block coded transmissions over frequency-selective fading channels," *IEEE Trans. Inf. Theory*, vol. 49, no. 1, pp. 164–179, Jan. 2003.
- [27] S. Zhou, B. Muquet, and G. B. Giannakis, "Subspace-based (Semi-) blind channel estimation for block precoded space-time OFDM," *IEEE Trans. Signal Process.*, vol. 50, no. 5, pp. 1215–1228, May 2002.



Xiaoli Ma (M'03) received the B.S. degree in automatic control from Tsinghua University, Beijing, China, in 1998 and the M.Sc. and Ph.D. degrees in electrical engineering from the University of Virginia, Charlottesville, in 1999 and the University of Minnesota, Minneapolis, MN, in 2003, respectively.

Since August 2003, she has been an assistant professor with the Department of Electrical and Computer Engineering, Auburn University, Auburn, AL. Her research interests include transmitter and receiver diversity techniques for wireless fading channels, communications over time- and frequency-selective channels, complex-field and space-time coding, channel estimation and equalization algorithms, carrier frequency synchronization for OFDM systems, and wireless sensor networks.



Geert Leus (M'97) was born in Leuven, Belgium, in 1973. He received the electrical engineering degree and the Ph.D. degree in applied sciences from the Katholieke Universiteit Leuven, in June 1996 and May 2000, respectively.

He was a Research Assistant and a Postdoctoral Fellow of the Fund for Scientific Research—Flanders, Belgium, from October 1996 to September 2003. During that period, he was with the Electrical Engineering Department, Katholieke Universiteit Leuven. Currently, he is an Assistant Professor with

the Faculty of Electrical Engineering, Mathematics, and Computer Science, Delft University of Technology, Delft, The Netherlands. During the summer of 1998, he visited Stanford University, Stanford, CA, and from March 2001 to May 2002, he was a Visiting Researcher and Lecturer at the University of Minnesota, Minneapolis. His research interests are in the area of signal processing for communications.

Dr. Leus received a 2002 IEEE Signal Processing Society Young Author Best Paper Award. He is a member of the IEEE Signal Processing for Communications Technical Committee and an Associate Editor for the IEEE TRANSACTIONS ON WIRELESS COMMUNICATIONS, the IEEE SIGNAL PROCESSING LETTERS, and the *EURASIP Journal on Applied Signal Processing*.



Georgios B. Giannakis (F'97) received the Diploma in electrical engineering from the National Technical University of Athens, Athens, Greece, in 1981. From September 1982 to July 1986, he was with the University of Southern California (USC), Los Angeles, from which he received the M.Sc. degree in electrical engineering in 1983, the M.Sc. degree in mathematics in 1986, and the Ph.D. degree in electrical engineering in 1986.

After lecturing for one year at USC, he joined the University of Virginia, Charlottesville, in 1987, where he became a Professor of electrical engineering in 1997. Since 1999, he has been a professor with the Department of Electrical and Computer Engineering, University of Minnesota, Minneapolis, where he now holds an ADC Chair in Wireless Telecommunications. His general interests span the areas of communications and signal processing, estimation and detection theory, time-series analysis, and system identification—subjects on which he has published more than 200 journal papers, 350 conference papers, and two edited books. Current research focuses on transmitter and receiver diversity techniques for single- and multiuser fading communication channels, complex-field and space-time coding, multicarrier, ultrawide band wireless communication systems, cross-layer designs, and sensor networks.

Dr. Giannakis is the (co-) recipient of four six paper awards from the IEEE Signal Processing (SP) Society in 1992, 1998, 2000, 2001, 2003, and 2004. He also received the Society's Technical Achievement Award in 2000. He served as Editor in Chief for the IEEE SIGNAL PROCESSING LETTERS, as Associate Editor for the IEEE TRANSACTIONS ON SIGNAL PROCESSING and the IEEE SIGNAL PROCESSING LETTERS, as secretary of the SP Conference Board, as member of the SP Publications Board, as member and vice-chair of the Statistical Signal and Array Processing Technical Committee, as chair of the SP for Communications Technical Committee, and as a member of the IEEE Fellows Election Committee. He has also served as a member of the the IEEE-SP Society's Board of Governors, the Editorial Board for the PROCEEDINGS OF THE IEEE, and the steering committee of the IEEE TRANSACTIONS ON WIRELESS COMMUNICATIONS.